Acta Pharmaceutica Sinica B 2024;14(11):4738–4755

Chinese Pharmaceutical Association
Institute of Materia Medica, Chinese Academy of Medical Sciences

Acta Pharmaceutica Sinica B

www.elsevier.com/locate/apsb
www.sciencedirect.com

REVIEW

Strategies for intravesical drug delivery: From bladder physiological barriers and potential transport mechanisms

Zheng-an Li [a,b], Kai-chao Wen [a,b], Ji-heng Liu [b], Chuan Zhang [a,*], Feng Zhang [b,*], Feng-qian Li [a,b,*]

[a]*School of Medicine, Shanghai University, Shanghai 200444, China*
[b]*Department of Urology/Pharmaceutics, Shanghai Eighth People's Hospital, Shanghai 200235, China*

Received 16 April 2024; received in revised form 28 June 2024; accepted 30 June 2024

KEY WORDS

Intravesical drug delivery;
Bladder cancer;
Transport barrier;
Carrier design;
Delivery mechanism;
Penetration;
Intravesical therapy;
Bladder

Abstract Intravesical drug delivery (IDD), as a noninvasive, local pathway of administration, has great clinical significance for bladder diseases, especially bladder cancer. Despite the many advantages of IDD such as enhanced focal drug exposure and avoidance of systemic adverse drug reactions, the effectiveness of drug delivery is greatly challenged by the physiological barriers of the bladder. In this review, the routes and barriers encountered in IDD are first discussed, and attention is paid to the potential internal/mucosal retention and absorption-transport mechanisms of drugs. On this basis, the avoidance, overcoming and utilization of the "three barriers" is further emphasized, and current design and fabrication strategies for intravesical drug delivery systems (IDDSs) are described mainly from the perspectives of constructing drug reservoirs, enhancing permeability and targeting, with the hope of providing systematic understanding and inspirations for the research of novel IDDSs and their treatment of bladder diseases.

*Corresponding authors.
E-mail addresses: zc843016@shu.edu.cn (Chuan Zhang), 1271774222@qq.com (Feng Zhang), fqlijr@126.com (Feng-qian Li).

Peer review under the responsibility of Chinese Pharmaceutical Association and Institute of Materia Medica, Chinese Academy of Medical Sciences.

https://doi.org/10.1016/j.apsb.2024.07.003

1. Introduction

The bladder is a vital dynamically functioning hollow organ in the body, responsible for the storage and excretion of urine[1,2]. Among the many urinary bladder diseases, such as cystitis, stones and tumors, bladder cancer (BC), which is overwhelmingly caused by the abnormal growth and proliferation of uroepithelial, is currently the leading cause of mortality and a serious threat to human health, with approximately 213,000 people dying of BC worldwide in 2020 alone[3]. Fortunately, the first diagnosis is not too bad in about 75% of BC patients, and the tumor has not yet invaded the muscle of the bladder wall or metastasized. These cases are classified as superficial/non-muscle-invasive bladder cancer (NMIBC). In contrast, other more aggressive tumors are diagnosed as muscle-invasive bladder cancer (MIBC)[4]. Although the combination of transurethral resection of the bladder tumor (TURBT) and periodic adjuvant chemotherapy or immunotherapy is used as the standard of clinical management, the rates of recurrence and progression of NMIBC are still concerning[5]. This is partially due to the fact that the effective drug dose reaching the lesion site is insufficient to eradicate the residual tumor cells after surgery[6]. Therefore, improvements in drug delivery methods are much needed to achieve therapeutic drug dosage.

Intravenous or oral administration is the major route of drug administration for tumor treatment. However, the effective drug accumulation at the target site is influenced by the first-pass metabolism, renal filtration, etc., and systemic adverse drug reactions cannot be avoided[7]. Systemic administrations appear to be unsuitable for drug delivery to the bladder, because the terminal organ: bladder, which is responsible for excretion, is relatively isolated and is challenging in the distribution of drugs. From this point of view, local administration, especially intravesical drug delivery (IDD), seems to be the best option for BC treatment. It allows one or more drug formulations to be instilled directly into the bladder *via* the urethra through a catheter or syringe, which significantly increases the effect of the drug onto the lesion, permits delivery in appropriate smaller doses and avoids systemic side effects[5]. Currently, IDD has been widely used in clinics as postoperative adjuvant therapy for NMIBC, and for MIBC, it has been used as the administration route of neoadjuvant therapy to reduce the pathologic rating and improve the patient's prognosis[8,9]. It is noteworthy that the combination of delivery drug-loaded carriers and IDD (Fig. 1A) has shown better results in terms of drug delivery, intra-tumor drug distribution and efficacy compared to intratumor injection (Fig. 1B) or systemic administration (Fig. 1C), and the proper design of drug delivery systems (DDSs) will endow IDD with many synergistic effects and special implications[10−12].

However, drugs imported *via* the urethra are subjected to dilution and elution by the continuously produced urine as well as affecting their stability. The presence of bladder permeability barriers and the lack of targeting of most drugs also limit effective drug delivery to lesions. The current intravesical instillation of conventional drugs still falls short in meeting the therapeutic demands for bladder diseases, particularly BC. In addition, reduced patient compliance due to discomfort of catheter insertion and multiple instillations should also be a concern[2]. This usually requires the preparation of the drug into carrier dosage forms such as nanoparticles or microspheres for localized/targeted and slow-released delivery. The delivery of therapeutic drugs and bladder physiopathology characteristics are particularly crucial considerations in the design of novel intravesical drug delivery systems (IDDSs). There are a series of strategies have been proposed to address the above delivery limitations, concerned around three main areas: (i) Prolonged residence time of drugs in the bladder. (ii) Enhancing penetration of the bladder permeability barrier. (iii) Empowering DDS with targeting. In this review paper, we introduce and analyze the route, three barriers and the associated transport mechanisms encountered by drugs in the IDD procedure. A more comprehensive understanding of the current progress of IDD-related research, such as system design, is provided to recognize a systematic foreword reference for IDDS research, as well as to offer new insights into the pharmaceutical treatment modalities of bladder diseases.

2. Intravesical drug delivery routes, barriers, and related mechanisms affecting transport

After reaching the bladder lumen, the transurethrally instilled drug molecules or DDSs firstly "stay" on the glycosaminoglycan (GAG)/mucus layer lining the inner wall of the bladder by adhesion and keep their physicochemical properties and spatial position relatively stable. Subsequently, the basal mucosa target site is reached with the aid of narrow paracellular (tight junction, TJ) or other potential transport pathways to overcome the epithelial or tumor tissue barrier. During this process, IDDS needs to face three physiobiological barriers (Fig. 2): urine in the lumen, mucus layer and epithelial/tumor tissue.

2.1. *Bladder lumen: Urine and periodic urination*

The bladder lumen is the environment where the drug first arrives after instillation through the catheter. The volume, composition and pH of the fluid in the lumen as well as the physiologic voiding response are primary factors to consider when designing IDDS. Although the average bladder capacity ranges from 400 to 500 mL, the detrusor receptors become stimulated, triggering the urge to urinate when the accumulation of urine delivered by the ureters in the lumen reaches 150−200 mL[1,13]. This is a major reason why IDD procedures make patients uncomfortable. On the other hand, because of the continuous production of urine and the flushing effect of urination, IDDSs are susceptible to dilution and have a short residence time at the site of the lesion. Response methods include increasing the provided dose, completely emptying the bladder before administration, limiting the patient's fluid intake or multiple administrations, to enhance passive diffusion based on the drug concentration gradient[14-16]. Adhesion strategy-based IDDSs (Please refer to Section 3.2), such as nanoparticles (NPs) and hydrogels, have been developed for the treatment of bladder diseases by adhering to the bladder lining to form a reservoir for sustained drug release, thereby providing locally high drug concentrations and resisting the effects of dynamic bladder activity, the dilution and flushing of urine.

Urine consists of 91%−96% water and rich solute components including metabolic end products (*e.g.*, urea, various amino acids), ions (*e.g.*, Ca^{2+}, Mg^{2+}), among others[17]. Because of filling, incomplete emptying and continued transport from the ureter, urine contact with the IDDSs is unavoidable. Then, stimulus-responsive IDDSs[18] and "motors"[19,20] have been developed with specific components in urine as response conditions or "fuels". Through urease-catalyzed decomposition of endogenous urea, the carbon dioxide gas generated enables self-propulsion of the nanomotor thus enhancing bladder penetration, while the toxicity possessed by the other product (ammonia) helps to kill tumor cells[19].

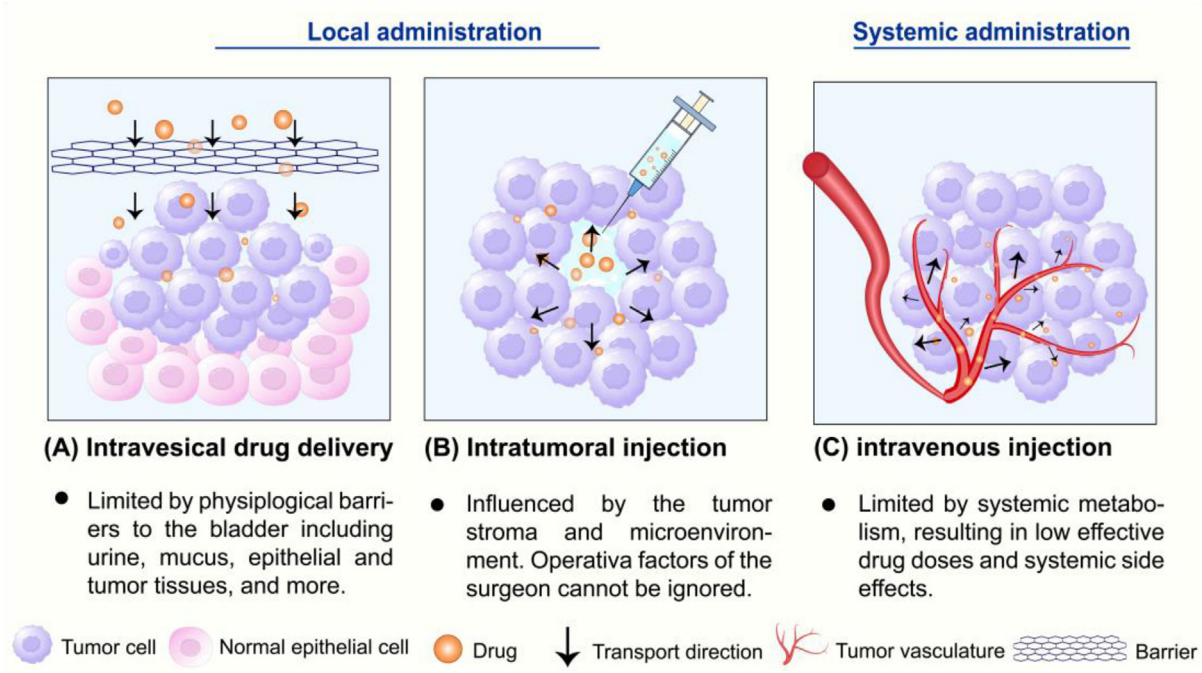

Figure 1 Drug delivery pathways, limiting factors and corresponding intratumor drug distribution patterns relevant to bladder cancer therapy. Local administration: (A) Intravesical drug delivery, where the drug crosses the glycosaminoglycan (GAG)/mucus layer barrier and diffuses layer by layer from the superficial tumor cells to the underlying tumor cells. (B) Intratumor injection, where the drug diffuses from the intratumor-injected liquid reservoir in all directions. Systemic administration: (C) Intravenous injection, where the drug diffuses from the vascular region of the tumor to the avascular region.

However, the urinary microenvironment also poses a challenge for researchers, as its composition, content and pH are influenced by a combination of factors such as diet, pathologic environment and circadian rhythms, which may potentially impact the stability of drugs or IDDSs[21]. For instance, the presence of nucleases (*e.g.*, ribonucleases) and cations in urine can potentially impact the efficacy of nucleic acid drugs with negatively charged, and for this reason, researchers have employed diverse drug carriers to enhance stability[22,23]. Differences in urine pH (which can vary from 4.5 to 8.0) may also result in drug release characteristics of carriers with pH-responsive properties not being as expected[24]. Therefore, the design of IDDS, especially the stimuli-responsive type, should take into account the individual differences in the content and pH of the components in the urine. Gellan gum, which

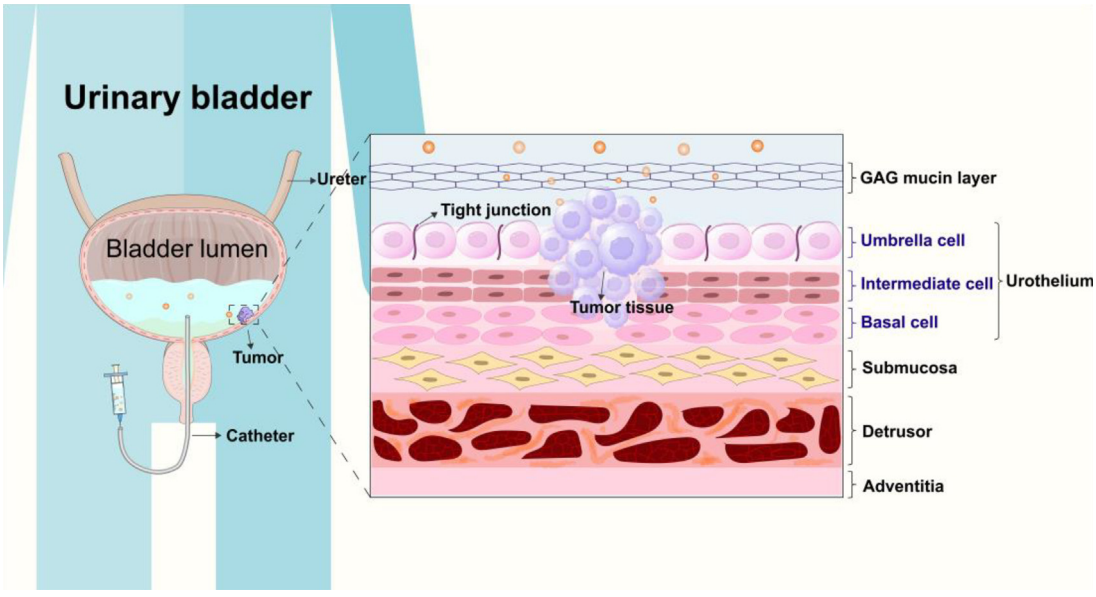

Figure 2 Schematic representation of the three physiologic barriers of the bladder encountered in IDD treatment of bladder cancer.

has cationic-triggered gelation characteristics and pH stability, has been chosen as the hydrogel material for the *in-situ* forming gel-liposome system[18]. It exhibits exceptional resistance to urine pH fluctuations and remains stable even in the pH 2.0−7.4 environment. Additionally, the urine can be treated before instillation (*e.g.*, taking medications, etc.) to ensure it consistent with the optimal environmental conditions for IDDSs.

2.2. GAG/mucus layer barrier

The bladder inner wall is lined with a hydrophilic elastic gel-like mucus layer about 10−20 μm thick, which is the first line of defense between urine and bladder tissue[25,26]. The cross-linked network composed of many mucus components (especially mucins) establishes a selective filtration barrier so that avoiding the reabsorption of harmful metabolites in the urine and protecting the underlying epithelium from bacterial invasion[27]. In addition, from the viewpoint of glycosylation, it is also known as the GAG layer because of its high content of protein-bound GAGs (*e.g.*, heparan sulfate, dermatan sulfate and chondroitin sulfate)[28,29]. Its permeability barrier function is based on two main mechanisms: size exclusion and interaction trapping (Fig. 3). Although not shielded from the dense 3D mesh pore, molecules smaller than the pore size may still be trapped due to their interactions (electrostatic, covalent, physical entanglement, etc.) with the mucus layer[30]. Therefore, considering the overall negative charge properties and the cysteine-rich hydrophobic structural domains of the mucus layer, drug carriers with hydrophilic, near-electrically neutral surface properties can significantly reduce the interaction trapping from mucus layer, while focusing the limiting factors for permeation on the size threshold[31,32]. The precise mesh size of the bladder mucus layer remains elusive, as it is equally influenced by various factors including pH and temperature. In a study conducted by Poinard et al.[31], the mesh size was described to be about 300 nm, and they demonstrated that two non-interacting/mucus-inert IDDSs with sizes ranging from 220 to 230 nm, namely polydopamine (PDA) coated polystyrene (PS) NPs and polyethylene glycol (PEG) coated PS NPs, exhibited excellent mucus diffusion behavior in the isolated porcine bladder model. Furthermore, photothermal or magnetothermal materials, mucolytic enzymes and self-propelled motors can be taken into account when designing mucus-penetration carriers, thereby alleviating the limitation on the mesh size of the mucus layer by altering or disrupting the mucus network structure in order to enhance the penetration behavior[12,33-35].

The content and composition of the GAG layer covering the BC tissues are altered compared to normal uroepithelium, and it is closely related to tumor grading and staging[36]. For example, the GAG layer in patients with higher-grade bladder cancer usually involves increased levels of chondroitin sulfate[37]. Given the major contribution of chondroitin sulfate to the permeability barrier function of mucus[38], Zhang et al.[32] in their review noted that the mucus layer covering the cancerous tissue was more impermeable than normal tissue.

2.3. Uroepithelial or tumor tissue barriers

The uroepithelium, which is located beneath and tightly bound to the GAG layer, consists of three main phenotypically distinct cell types: basal, intermediate, and superficial/umbrella cells (Fig. 2). Among them, the umbrella cells located in the most superficial layer have the highest degree of specialization, are arranged in a hexagonal shape, have insoluble polarized membranes, are relatively large and can achieve a stretch of 50−120 μm depending on the filling of the bladder[13]. The barrier properties of the uroepithelial tissue are contributed by TJs between umbrella cells and by dense plaques that almost cover their apical surfaces, the so-called asymmetric unit-membrane special structures so that preventing the reabsorption of metabolic wastes in the urine[39]. The presence of cytoskeletal fibers allows further enhancement of the barrier properties as they are able to attach to the TJ of the basolateral membrane[40].

Notably, typically BC follows an outward growth pattern and lacks TJs relative to normal uroepithelium due to poor specialization, implying some passive targeting of drug delivery[41]. Therefore, BC cell uptake and how to pass through the dense accumulation of BC cells and extracellular matrix layer by layer from the luminal surface where the tumor tissue is located to reach the deep tumor tissue is the second challenge faced by IDDSs after overcoming the GAG layer. Several drug delivery strategies have

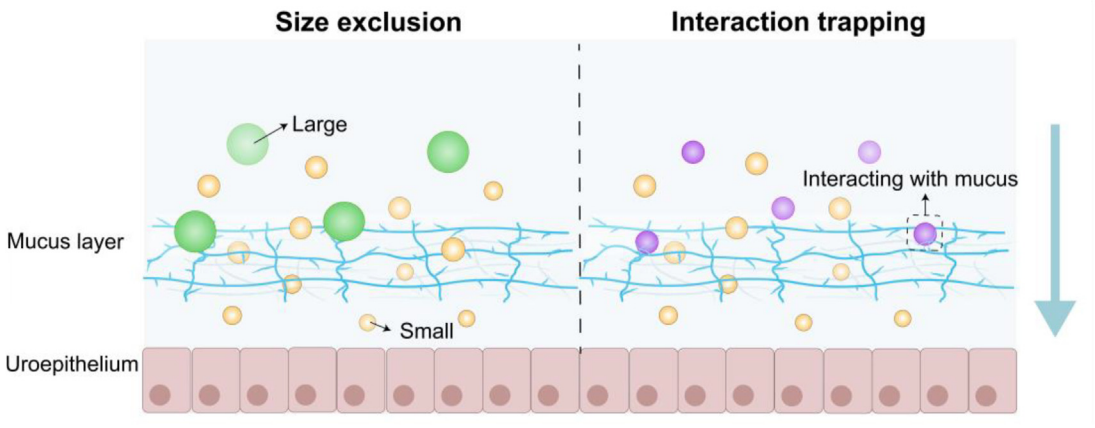

Figure 3 Schematic representation of the GAG/mucus layer barrier mechanism, including size exclusion and interaction trapping. Particles larger than the mucus pore size (green) are excluded from the mucus crosslinking network, while smaller particles can pass through. The particles (violet) are trapped on the surface of the mucus layer due to their interaction with the mucus and are unable to reach the underlying epithelial tissue. These interactions include electrostatic, covalent, hydrophobic, macromolecular entanglement, etc.

been attempted, targeting potential transport mechanisms of DDSs to improve BC cell internalization and tissue penetration. Those can be classified as paracellular and transcellular transport (Fig. 4).

Paracellular transport (Fig. 4A) is actually simple passive diffusion based on the concentration gradient in the extracellular matrix and the strategies to enhance it involve adjusting the size as well as the use of TJ modulators so that DDSs can pass through the BC cells gap[42,43]. Transcellular transport includes direct cell-to-cell transfer (Fig. 4B) and transcytosis (Fig. 4C). Direct transfer of intracellular cargo between two adjacent or distant cells can be achieved by direct contact or by forming gap junctions and tunneling nanotubes[44-47]. Transcytosis, on the other hand, realizes the indirect intercellular transfer of cargoes crossing the extracellular matrix through endocytosis and exocytosis processes, and the related mechanisms involve electrostatic adsorption, receptor and transporter protein-mediated. The former (Fig. 4c1) can be triggered by DDSs with positively charged surfaces that are capable of electrostatic interactions with negatively charged cell membranes, while the latter two (Fig. 4c2 and c3) are usually dependent on the assembly of specific ligands or transporter recognition units in the DDS[48,49].

The prerequisite for triggering the above transcellular transports is that IDDS needs to be internalized by the cell first. In most cases, the entry of nanoscale DDS into cells is dependent on endocytosis, which is also commonly associated with transcytosis[50]. Another pathway of cellular internalization involves direct fusion with the plasma membrane, and the triggering of this pathway is related to specific lipid components contained in the DDS[51]. Inspired by the cytotoxic ammonia generated from urea catalyzed by urease, Jing et al.[52] proposed a strategy to redesign tumor cell membranes using urea transporter protein-B (UT-B) to facilitate urea transport to tumor cells and the accumulation of ammonia in tumor cells. The biomimetic fusogenic liposomalized nanoporter which they constructed can load UT-B into tumor cell membranes in a membrane fusion manner, while urease is delivered into the cytoplasm. This ingenious idea facilitates cellular internalization or transport screening of therapeutic substances by creating "gates" (*e.g.*, transporter proteins) in the membranes of target cells.

Based on the above analysis of the three major barriers encountered during IDD, the corresponding effects on the drug stability and the possible transport mechanisms, the current design strategies and practices of IDDSs that can effectively overcome barrier effects will be presented and elaborated below.

3. Strategies for prolonging residence time: Building drug reservoirs

Whether considered in terms of the removal of IDDSs by physiologic voiding or patient discomfort due to catheter insertion or multiple drug administrations, the construction of *in situ* drug reservoirs to prolong the residence time of IDDSs in the bladder or at the target site is necessary. Depending on the location of reservoirs, these strategies were categorized into three groups: Urine floating (within the bladder lumen), adhesion (on the surface of the bladder lining), and lysosomal escape (within BC cells).

3.1. *Urine floating*

"Floating", the well-known strategy, is usually applied to the construction of gastric retention DDSs, and recently it has also been extended to IDD (Table 1)[53-59]. These IDDSs with low densities can float in the urine that accumulates in the bladder

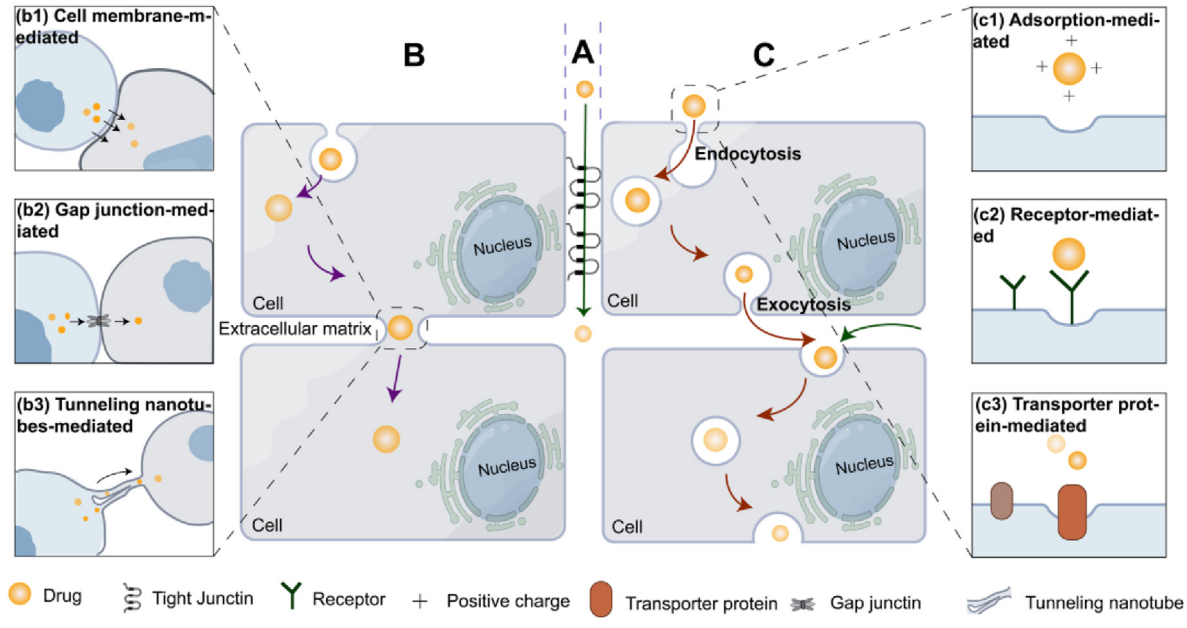

Figure 4 Potential mechanisms of drug transport in uroepithelial or cancer cells, including paracellular (A) and transcellular transport (B, C). (A) Paracellular transport, in which drugs cross from the tight junction between two neighboring cells. (B) Direct cell-to-cell transfer, which can be mediated by cell membranes (b1), gap junction (b2), and tunneling nanotubes (b3). Drugs are transferred directly between two cells without passing through the extracellular matrix. (C) Transcytosis, which can be mediated by adsorption (c1), receptor (c2) and transporter proteins (c3). Drugs are *trans*-ported between two cells by endocytosis and exocytosis processes that require passage through the extracellular matrix.

Table 1 Various floating IDDSs in terms of key components and fabrication methods.

System	Cargo	Key component	Fabrication method	Annotation	Ref.
P407-bases floating hydrogel	Dox-load HAS NPs	P407 (35%, *w/v*); HPMC (5%, *w/v*); $NaHCO_3$ (6%, *w/v*)	Gas-producing agent	$NaHCO_3$ produces CO_2 gas under acidic conditions.	53
	Dox	P407 (45%, *w/v*); NH_4HCO_3 (6%, *w/v*)	Gas-producing agent	Thermal decomposition of NH_4HCO_3 at physiological temperature to NH_3, CO_2 and H_2O.	54
	Dox	P407 (45%, *w/v*); PFP (10%, *w/v*)	Gas-producing agent	Vaporization of PFP at physiological temperatures due to its low boiling point (29.2 °C).	55
	RhB	P407 (45%, *w/v*)	Shaking or stirring	The ability of P407 to self-generating microbubbles by shaking.	56
BSA air microbubbles	Dox	BSA (20%−50%, *w/v*)	Freeze-drying	Density reduction and volume expansion when water is converted to ice.	57
Multi-layered chitosan-alginate hydrogel capsules	Calcium carbonate powder Fe_3O_4 NPs	Chitosan; Sodium alginate Calcium chloride; Pluronic F-127	Magnetism-assisted bubbling	Magnetically driven deformation of a thin hydrogel film and formation of bubbles.	58
PLGA-based floating controlled-release DDSs	Dox; IR780	PLGA (20%, *w/v*)	Shaking or stirring	The internal honeycomb structure of the prepared DDS allows for suspension in water.	59

P407, poloxamer 407; Dox, doxorubicin; HAS, human serum albumin; HPMC, hydroxypropyl methylcellulose; PFP, perfluoropentane; RhB, rhodamine B; BSA, bovine serum albumin; DMAC, dimethylacetamide; PLGA, poly(lactic-*co*-glycolic acid); NPs, nanoparticles; DDSs, drug delivery systems.

lumen, providing a sustained and slow release of drugs and reducing the risk of urinary tract obstruction. The secret of "floating" lies in their loose, cavity-filled (honeycomb) structure. Based on the method of cavity formation, they are broadly classified into four categories: (i) addition of gas-generating agents, (ii) simple oscillation and stirring, (iii) freeze-drying, and (iv) magnetically assisted bubbling.

Based on the CO_2 gas production property of $NaHCO_3$ under acidic conditions and the temperature-sensitive property of P407 hydrogel, Lin et al.[53] constructed a floating hydrogel system. When it enters the bladder environment, P407 achieves the sol−gel transition in response to physiological temperature, while $NaHCO_3$ produces gas to confer the honeycomb-like structure to the gel. However, the prerequisite for floating is acidification of the urine prior to administration. To overcome this limitation and avoid the potential irritation caused by low pH, they subsequently improved by replacing $NaHCO_3$ with NH_4HCO_3, which can be thermally decomposed at 37 °C to produce two gases of NH_3 and CO_2[54]. Similarly, Zhu et al.[55] used perfluoropentane, which has the ability to vaporize at body temperature due to its low boiling point, as the gas-generating agent and the contrast agent for P407 floating hydrogel. It has the advantages of strong stability, reaction inertness and visualization-monitoring compared to the chemical reaction-based $NaHCO_3$ and NH_4HCO_3.

The method of forming cavities during gel formation by introducing air through oscillation, stirring or homogenization to obtain floating properties may be the most convenient and practical, which usually requires the addition of an emulsifying/foaming agent component to the prescription. The nonionic surfactant P407 itself has the property of self-foaming and can be oscillated to form air-encapsulated micelles in order to obtain floating hydrogels[56]. After three urination processes, its drug release in the rabbit bladder model still managed to reach 12.5%, effectively prolonging its residence time in the bladder.

Unlike the methods of *in situ* molding in the bladder lumen described above, the freeze-drying and magnetically assisted bubbling methods require the construction of the floating IDDS to be completed before the bladder instillation procedure. The surface cross-linking-freeze-drying method (Fig. 5A) was employed in the construction of floating bovine serum albumin microbubbles (BSA-MBs) loaded with doxorubicin (Dox)[57]. Because the principle of cavity formation by freeze-drying is based on the volume expansion of water when it is converted to ice, an aqueous core needs to be created inside the carrier first. Core-shell structured microcapsules with BSA aqueous solution as the core were obtained by W/O emulsification and surface cross-linking. Subsequently, they were freeze-dried. During the conversion of the aqueous core into ice crystals and sublimation, the cavity, which was larger than the original aqueous core, and the protein layer covering the inner surface of the cavity were formed, thus obtaining the three-layer structured carrier (cavity-protein layer-shell) with floating properties. Compared with conventional bilayer-structured microbubbles, the presence of an intermediate protein layer greatly enhanced drug loading and structural stability. The drug encapsulation efficiency of BSA-MBs was >95%, and the drug loading efficiency was 15.8%. Even after 5 days of artificial urine incubation, the cavity size did not change much and about 80% of the BSA-MBs retained the ability to float.

Magnetic-assisted bubbling method, in which the magnetically driven stretching deformation of the gel liquid film is utilized to

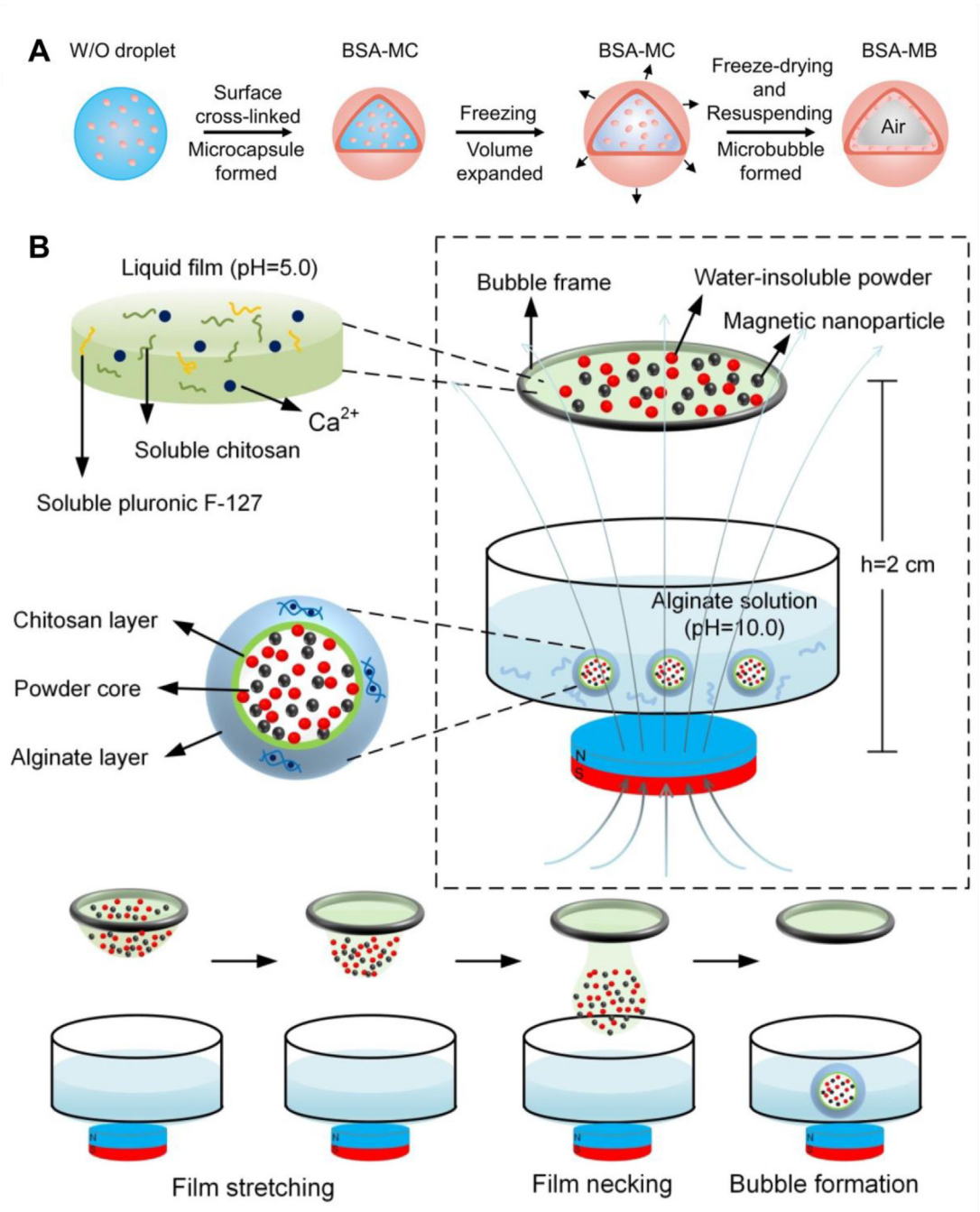

Figure 5 Example diagrams of the preparation of floating IDDSs by freeze-drying and magnetic field-assisted bubbling methods. (A) Fabrication route for BSA-MBs by freeze-drying method. Reprinted with the permission from Ref. 58. Copyright © 2022 Elsevier. (B) Fabrication route for multilayered chitosan-calcium alginate hydrogel capsules by magnetically assisted bubbling. Reprinted with the permission from Ref. 59. Copyright © 2023 WILEY.

encapsulate air to form bubble-based cavities (Fig. 5B). This method was proposed when Liu et al.[58] constructed multilayered chitosan-calcium alginate hydrogel (MP/H) capsules co-loaded with water-insoluble powder and Fe_3O_4 magnetic NPs. A hydrogel liquid film comprising chitosan, P407 and $CaCl_2$ was attached to the bubbling frame located above the pool containing the alginate solution. Driven by both magnetic and gravitational force, Fe_3O_4 magnetic NPs and water-insoluble powders are co-encapsulated in bubbles created by the deformation of the liquid film. As the bubbles fall, Ca^{2+} interacts with the alginate, thereby attaching an outer layer of calcium alginate gel to the surface of the chitosan bubbles. In particular, they note that this magnetically-assisted bubbling-coating step can be repeated to obtain multilayer structures. In a bladder-simulating container, the MP/H capsule showed good floating and magnetoconductivity and possessed three-stage release behavior and >175 h slow-release capability.

Notably, although floating reduces the risk of urinary tract obstruction, floating IDDSs are also more affected by external factors such as the pH, volume and composition of the urine, and torso posture. Therefore, in addition to good floating properties to resist the scavenging effects of physiological voiding activity, an ideal floating IDDS should be stable in the bladder lumen environment and have sustained drug release behavior.

3.2. *Adhesion of bladder lining*

Bio-adhesive IDDSs are able to adhere to mucus or cells on biological surfaces (bladder lining) and thus can be subdivided into cell adhesion and mucus adhesion. Adhesion strategies that specifically aim at cancer cells can also be referred to as targeting strategies and will be discussed in subsequent Section 5. This section focuses on mucus adhesion.

Unlike the gastrointestinal mucus, which exhibits relatively predictable and rapid turnover rates, the bladder mucus layer does not appear to be a dynamically secreted barrier and is subject to urination[25,60]. It is tightly bound to the underlying umbrella cell membrane, which is slow to renew, favoring the long-term residence of adherent IDDSs in the bladder lining. The mechanism of adhesion lies in the complex interactions formed between IDDS and mucus, including electrostatic, lectin-sugar, physical chain entanglement, covalent and other interactions. Table 2[23,61-68] summarizes the surface modification strategies and corresponding mechanisms of current adherent IDDSs.

The mucus, which exhibits overall negative electrical properties, can electrostatically adsorb IDDSs with positively charged surfaces. Therefore, the electrostatic adhesion strategy was aimed at conferring cationic groups (*e.g.*, amino groups) on the DDS surface. Chitosan[61] and poly(amidoamine) (PAMAM) dendrimers[62], which are amino group-rich, have been used as surface coatings on nanodiamonds and mesoporous silica nanoparticles (MSN) for intravesical delivery of Dox, respectively. A series of MSNs coated with G0−G3 PAMAM, respectively, were prepared, and the results of adhesion studies based on mucin and isolated porcine bladders showed that the adhesion performance of G2 PAMAM was stronger than that of G0 and G1 PAMAM, which demonstrated that the adhesion capacity of the bladder lining was positively correlated with the number of amino groups in PAMAM. For G2 and G3 PAMAM, there was little difference in adhesion performance, which Wang et al.[62] hypothesized was due to saturation of the mucin binding site.

Lectins, which represent the second generation of bio-adhesive materials, have been used to confer specific adhesion to DDS's surfaces due to their ability to interact with specific glycosyl sequences in the structural domain of the mucus-glycocalyx[69,70]. Several specific glycosylation receptors of lectins have been identified in normal and malignant uroepithelia, with wheat germ agglutinin (WGA) and Concanavalin A (ConA) being the most widely used in IDDSs[71-73]. Moreover, because of the overexpression of WGA- and ConA-binding receptors in BC, they can provide tumor targeting while mediating bio-adhesion. WGA-functionalized PLGA NPs loaded with *N*-acyl-gemcitabine have been developed for the intravesical treatment of tumors[64]. After studying the glycosylation status of human and murine bladder cancer lines using a "focused" lectin array, Hou et al.[73] selected ConA as the functional lectin. The ConA-epirubicin coupling linked by a pH-sensitive connector showed high binding to cancer cells and enhanced antitumor activity in the BC mouse model.

The surface roughness topology contributes to enhanced mucus adhesion of the particles, which can be provided by modifying its surface with long-chain polymers, whereby physical chain entanglements can be formed with the mucus layer. Wang et al.[65] calcined hollow silica nanoparticles at 550 °C and modified them using Silane−PEG−NH_2 to obtain what they called the pollen-like rough surface. The pollen-like structure nanoparticles exhibited significant accumulation in the bladder of the *in situ* BC mouse model compared to the simple nanoparticles. Besides long-chain PEG and its derivatives, polyacrylic acid or carbomer junctions can also be used to enhance adhesion, although their use in IDD has not been reported[60].

Covalent bonds appear to provide stronger adhesion than that provided by physical entanglement or non-covalent interactions. Mucosal mucins have cysteine-rich subdomains that can react with IDDSs modified with certain groups on the surface (*e.g.*, sulfhydryl groups, maleimides, catechols, etc.) under physiological conditions in order to form covalent bonds (Table 2). Chen et al.[63] used 3-mercaptopropyltrimethoxysilane (MPTMS) as the sulfhydryl provider for sulfhydryl functionalization of the MSN surface so that it could be firmly attached to the bladder lining by forming disulfide bonds. Notably, they also found that thiolated MSN exhibited a more enhanced drug penetration ability in Caco-2 and MBT-2 cell monolayer models, with the apparent permeability coefficient being 4.25-fold higher than that of unmodified MSN. This permeation-enhancing effect results from the modulation of the mucosal reduced/oxidized glutathione (G−SH/G−S−S−H) ratio by the sulfhydryl/disulfide bond exchange reaction, as increased G−SH levels help to open TJ[63,74].

The adhesive IDDSs mentioned above mostly adhere to the bladder lining in the form of nanoparticles. Other carrier types include polymer gels[18,75] and transformable nanoparticles[76] based on self-assembled peptides, which can form *in situ* 3D fibrous networks firmly bound to the bladder wall or solid tumor surface. However, attention needs to be paid to their risk of interfering with urinary flow, causing irritation and urinary tract obstruction during adhesion and detachment.

3.3. *Lysosomal escape-based intracellular reservoirs*

The endo/lysosomal route is the most common route of entry into cells for nano-delivery systems, which means that they (especially those used to deliver drugs that need to be active in cytoplasmic or subcellular compartments) are often faced with endo/lysosomal traps[77,78]. In addition, it cannot be excluded that DDSs leave the cells or diffuse through the blood vessels to other organs before the effective number of drugs has been released[78]. Intracellular reservoirs were constructed to enhance DDSs' residence time at the tumor site. They usually have the ability to escape from endo/lysosomes and self-assemble within tumor cells to form reservoirs that continuously release drugs.

Zeng et al.[78] reported a hydroxycamptothecin (HCPT)-peptide prodrug that can be triggered to self-assemble by the enzyme cathepsin B (CtsB) overexpressed in the cytoplasm of bladder tumors. Its self-assembly responsiveness is derived from the portion of FF peptide, which has a high self-assembly propensity, and the portion of GFLG peptide, which can be recognized and cleaved by CtsB. With the help of nonaethylene glycol (HO−PEG_9−OH), Dox was linked to 3−aminopropyltriethoxysilane to form Dox-silane conjugate and then self-assembled to form prodrug nanoparticles[79]. The presence of silanes allows them to hydrolyze in response to the lysosomal acidic environment thereby initiating the

Table 2 Surface modification strategies for adhesive IDDSs.

Surface strategy	Provider	Carrier	Cargo	Mechanism	Annotation	Ref.
Amino group	Chitosan	Nanodiamonds	Dox	Electrostatic interaction	Surface amines provide a positive charge and thus interact with negatively charged mucus.	61
	PAMAM	MSN	Dox			62
	DSPE−PEG−NH_2	PLGA NPs	KDM6A-mRNA			23
Thiol group	DSPE−PEG−SH			Covalent interaction	Thiol/disulfide exchange reactions with cysteine-rich mucin substructures of mucus mucins.	
	MPTMS	MSN	MMC			63
Lectins	WGA	PLGA NPs	*N*-Acyl-gemcitabine	Lectin-sugar interaction	Specific binding to specific carbohydrates which expressed in the mucus-glycocalyx structure.	64
Long chain polymer	Silane−PEG−NH_2	Hollow silica NPs	Pirarubicin	Macromolecular tangle	Empowering DDSs with surface roughness topology.	65
Mal group	PLGA-PEG−Mal	PEG-PLGA NPs	−	Covalent interaction	Michael addition reaction with thiols on cysteine-rich mucins.	66
	MHA	Chitosan-alginate NPs	Dox			67
Catechol group	Dop			Covalent interaction	Schiff base or Michael addition reactions with primary amine groups and thiol groups in mucus.	
Methacrylate group	MA	Chitosan NPs	−	Covalent interaction	Michael addition reaction with thiols on cysteine-rich mucins.	68

−, not applicable.
PAMAM, poly(amidoamine); MSN, mesoporous silica nanoparticles; PEG, polyethylene glycol; DSPE-PEG, 1,2-distearoyl-*sn*-glycero-3-phosphoethanolamine-conjugated PEG; MPTMS, 3-mercaptopropyltrimethoxysilane; MMC, mitomycin C; MHA, 6-maleimidohexanoic acid; Mal, maleimide; DOP, dopamine hydrochloride; MA, methacrylic anhydride; Dox, doxorubicin; PLGA, poly(lactic-*co*-glycolic acid); NPs, nanoparticles; DDSs, drug delivery systems.

escape program and to condense in response to the neutral environment upon entry into the cytoplasm thereby forming the intracellular nano-reservoirs.

However, the strategy of constructing intracellular reservoirs to prolong tumor tissue residence time alone has minimal effect on how other barriers (physiological urination, mucus layer, etc.) are breached during IDD. Combining with other strategies for IDD or using intra-tumor injection for drug delivery may be a better option.

4. Non-specific strategies to enhance penetration

4.1. Non-interaction strategy

In contrast to the mucus adhesion strategy, the non-interacting strategy aims at escaping from the interaction-based trapping in the mucus layer by precisely tuning the surface properties of the DDSs so that they can diffusely penetrate through the mucus layer in a fast and "slippery" manner. The prevailing approach involves endowing DDSs with hydrophilic and electrically neutral surface properties to evade hydrophobic−hydrophobic and electrostatic interactions, which are also based on the mimicry of viruses with mucus-permeable escape capabilities in nature.

Hydrophilic, neutral polymers represented by PEG have been incorporated into the formulation of mucus-inert DDSs[80,81]. The high-density PEG coating enhances mucus penetration by shielding the charge of the nanocarriers and forming a surface hydration layer through hydrogen bonding. It is important to note that a prerequisite for mucus inertness by this method is the high-density coating of low molecular weight PEG, otherwise, the long polymer chains may entangle with the mucus and cause adhesion, which is the opposite of the desired effect. Wang et al.[81] developed surface-coated PS nanoparticles with different molecular weight PEGs and found that the molecular weight interval for the inert−adhesion transition of PEG was 5−10 kDa.

An alternative approach to achieve mucus inertness is to impart the high-density anionic and cationic groups on the surface of DDSs and adjust the overall surface charge to a neutral or slightly negative ζ-potential. Due to the overall near-neutral ζ-potential as well as electrostatically induced hydration (ionic solvation), such DDSs show similar or stronger anti-mucus adsorption ability than hydrophilic coatings based on hydrogen bonding (*e.g.*, PEG)[31,82]. Specific measures include the combination of anionic and cationic

materials and the use of zwitterionic polymer coatings[83,84]. Notably, mucus penetration efficiency is affected by the surface space charge distribution. By examining the mucus transport behavior of two peptides with the same net charge but with different arrangements of positive and negative charges (separated and staggered), Li et al.[85] found that the peptide with staggered positive and negative charges exhibited better mucus-inert behavior. Therefore, balanced charge distribution is one of the prerequisites for good mucus-inert behavior of DDSs based on high-density charged surfaces. In this respect, zwitterionic polymer coatings may be more advantageous.

However, the hydrophilic, near-electrically neutral surface properties may be detrimental to further tumor cell uptake of DDSs. Thanks to the unique hydrophobic and lipophobic phase-separation properties derived from fluoro-carbon chains, fluorinated polymers have become suitable carriers for transmucosal delivery of macromolecules such as genes and proteins, exhibiting effective *trans*-mucous permeation, cellular internalization and endosomal escape[86-88]. Fluorinated chitosan (FCS) prepared by grafting perfluoroheptanoic acid onto chitosan has been used as the delivery carrier for catalase-coupled meso-tetra(4-carboxyphenyl)porphine (TCPP), an acoustic sensitizer[89]. Transwell assay and flow cytometry results showed that the use of fluorinated chitosan significantly enhanced tissue permeability and cellular uptake behavior. In addition, its endosomal escape ability was improved, with the percentage of lysosomal co-localization signals being one-third of that of the chitosan group without fluoride modification.

4.2. *Break the barriers*

If there's no way to bypass the barrier, then just break it. Corresponding methods include physical methods, such as Electromotive drug administration (EMDA) and photothermal therapy, and chemical methods, such as the use of mucolytic enzymes and TJ modulators.

EMDA is actually an intravesical bladder device adjuvant therapy that applies a small electric to the bladder wall through the catheter equipped with internal electrodes so as to enhance drug *trans*-epithelial penetration[90]. However, most current EMDA-based studies only involve the delivery of pure drugs (*e.g.*, mitomycin) and commonly used drugs for BC treatment have little tumor selectivity. There is also a possibility that EMDA procedure may damage the structure of drugs. Photothermal therapy (PTT) has shown advantages in the BC treatment *via* IDD procedures, with the aid of the response-heat of the photothermal agent at specific laser wavelengths, DDSs can break mucous, urothelium barrier and the solid tumor tissue barrier by thermal ablation[10,91-93]. To avoid detachment from the bladder wall before laser irradiation as well as inadvertent injury to normal tissues, DDSs based on PTT should also have a certain degree of adhesion and tumor targeting. Yang et al.[92] developed a targeted gold nanorod photothermal ablation DDS for the intravesical treatment of BC. Anti-epidermal growth factor receptor (EGFR) is overexpressed on the luminal surface of the bladder tumor, and therefore gold nanorods coupled with anti-EGFR antibodies (CNRs) can be specifically bound to the luminal surface of tumors to allow for subsequent PTT under laser irradiation.

Typical examples of chemical methods to enhance mucus permeation are the use of mucolytic enzymes, as they can partially break down the three-dimensional meshwork of mucins[94]. Based on the ability of papain to cleave the internal amide bond (peptide bond) of the mucin amino acid sequence, one research[34] co-encapsulated it with gemcitabine in the hydrogel prepared from gellan gum or sodium carboxymethyl cellulose (CMC). The hydrogel acts as an adhesive drug reservoir on the bladder wall, while papain dissolves the mucus to improve drug *trans*-bladder tissue penetration. Compared to enzyme-free nano-formulations, CMC hydrogels containing natural papain exhibited the strongest drug bladder penetration. Other enzymes that can cleave amide bonds are trypsin, bromelain, proteinase K, etc.[94] In addition, the mucus network is enriched with disulfide bonds, and therefore the breaking of disulfide bonds using a disulfide bond reducing or exchange agent, such as *N*-acetyl-L-cysteine, is also a way to enhance mucus permeation[95]. However, with the exception of papain, these mucolytic agents have not been used in IDD research.

Another way to promote permeation acts on the TJ because it contributes significantly to the barrier function of urinary epithelial cells, thus adjusting the pore size in TJs can facilitate the paracellular transport of drugs or molecules. Traditional nonspecific TJ modulators include bile salts, Ethylene Diamine Tetraacetic Acid (EDTA), ethylene glycol tetraacetic acid (EGTA), and sodium decanoate[42,96]. The natural chitin-derived cationic polymer chitosan and its derivatives have become popular carrier and coating materials for IDDSs due to their ability to transiently open the TJ between epithelial cells, electrostatic adsorption with the mucus layer, biocompatibility, degradability, and low cost[97]. Sun et al.[43] used magnetic thermosensitive chitosan/β-glycerophosphate hydrogel as the intravesical deliver carrier of pirarubicin. By examining the transcript levels of common TJ-related genes in bladder cancer cells, they found that chitosan modulates TJ by decreasing occludin expression. In another research[98], polymer-lipid hybrid nanoparticles consisting of *N*-(2-ethylamino)-6-*O*-glycol chitosan and 1,2-dioleoyl-*sn*-glycero-3-phosphoethanolamine were used for localized intravesical gene delivery, and the IDDSs was effective at penetrating the bladder barrier and facilitating the intrinsic layer uptake of genes.

It should be noted that these strategies based on barrier-breaking may lead to irreversible changes in the associated barrier function, and prolonged exposure may also cause unexpected side effects such as interstitial cystitis.

4.3. *Self-propelled micro/nano-motors*

With the ability to convert energy provided by chemical fuel-based catalytic reactions or external fields (*e.g.*, magnetic, acoustic, light, etc.) into mechanical motion, micro/nano-motors (MNMs) can move on their own in liquids and across biological barriers at controlled speeds and trajectories so as to deliver drugs to the target region which is located deep in the bladder (Table 3)[99-105].

Because of the high concentration of urea ($\sim$300 mmol/L) in the urine after renal excretion, MNMs driven by enzymatic conversion of endogenous urea have been extensively studied in IDD[99-101]. For example, Hyunsik et al.[101] produced nanomotors (Ur-PDA NC) that could self-diffusively propel in urine by modifying the surface of hollow polydopamine nanoparticles with urease. The self-diffusive propulsion capability originates from the unbalanced catalytic reaction of urease molecules on the motor's surface. In contrast to the random Brownian motion of non-urease functionalized nanomotors in urine, Ur-PDA NC displayed low urea concentration-dependent, high urea concentration-saturated speed and directionality, and exhibited

Table 3 Various self-propelled micro/nano-motors for IDD.

Energy source	System	Cargo	Key ingredient	Annotation	Motion analysis	Ref.
Biofuel	Self-driven urease-HSA proteomotors	MSO	Urease	Urease-catalyzed urea decomposition; MSO inhibits the conversion of amines from toxic to non-toxic.	Diffusion coefficient: 1.46 μm^2/s (urea concentration: 50 mmol/L).	99
	Anti-FGFR3 antibody-modified MSN NPs	–	Urease; Anti-FGFR3 antibody	Urease-catalyzed urea decomposition; Anti-FGFR3 antibody provides tumor targeting ability.	Diffusion coefficient: approximately 0.84 μm^2/s (urea concentration: 40 mmol/L).	100
	Polydopamine hollow NPs	–	Urease	Urease-catalyzed urea decomposition.	Speed: 10.67 μm/s (urea concentration: 100 mmol/L).	101
	Janus platelet micro-motor	Dox or Cip	Urease	Urease-catalyzed urea decomposition.	Speed: approximately 6 μm/s (urea concentration: 100 mmol/L).	102
Magnetic field	cRGD and Fe_3O_4 NPs modified Janus 293T cell robots	OV	Fe_3O_4 NPs; cRGD	Fe_3O_4 NPs provide magnetic field responsiveness; cRGD provides tumor targeting capability.	Speed: 44.4 μm/s at 10 Hz, 10.3 mT.	103
Acoustic field	Microrobots with symmetric fins and mushroom-shaped cavities	DEX	–	Self-propulsion through oscillation of trapped bubbles at their resonant frequency.	Speed: approximately 150 body lengths per second at 320 kHz.	104
Light	Self-assembled [FeFe] TPP/FCS NPs	GEM	[FeFe]TPP	Photocatalytic release of hydrogen from [FeFe] TPP.	Speed: 10.67 μm/s (urea concentration: 100 mmol/L).	105

–, not applicable.
MSO, L-methionine sulfoximine; FGFR3, fibroblast growth factor receptor 3; GEM, gemcitabine; Cip, ciprofloxacin; OV, oncolytic viruses; cRGD, cyclic arginine-glycine-aspartic acid tripeptide; DEX, dexamethasone; [FeFe]TPP, [FeFe]-hydrogenase; FCS, fluorinated chitosan; HAS, human serum albumin; MSN, mesoporous silica nanoparticles; Dox, doxorubicin; NPs, nanoparticles.

bladder tissue penetration to a depth of 60 μm at 12 h after intravesical instillation in mice. In the research of ANA et al.[106], the combination technology, positron emission tomography-computed tomography (PET-CT), was used to analyze the *in vivo* and *ex vivo* swarming behavior of urease-powered mesoporous silica nanomotors. The results show that, unlike the non-uniform two-phase distribution of passive particles, urease-powered nanomotors move in clusters and exhibit enhanced fluid mixing characteristics in the mouse bladder. What's more, the potential antitumor effects of toxic ammonia, the urea-catalyzed product of urease-powered MNMs, deserve attention. However, biotransformation-based detoxification processes prevent the maximum utilization of ammonia toxicity, therefore the glutamine synthetase inhibitor, L—methionine sulfoximine, was loaded into the urease-powered human serum albumin motors to amplify ammonia's anticancer toxicity by inhibiting ammonia metabolism (the conversion of toxic ammonia to nontoxic glutamine)[99].

The barrier penetration properties of MNMs are highly dependent on the effectiveness of their directed propulsion, and the breaking of symmetry is the key to controlling their more efficient directed propulsion, which can be achieved by the asymmetric immobilization of enzymes or other active components that can responsive to external stimuli (magnetic field, sound, light, etc.) on the surface of MNMs. Tang et al.[102] obtained Janus-structured MNMs by asymmetrically immobilizing urease on the platelet surface. At the same fuel (urea) concentration, Janus-structured MNMs exhibited more efficient motility, with an effective diffusion coefficient approximately 2 times that of non-Janus MNMs. Janus-immobilization of Fe_3O_4 NPs on the surface of cRGD-modified 293T cell robots enables fuel-free, controlled targeted penetration of 3D tumor spheroids powered by the external rotating magnetic field thereby delivering engineered oncolytic viruses to deep tumor tissues[103].

The effect of surface structure on the trajectory of MNMs is also reflected in the work of Lee et al.[104] they used two-photon lithography to 3D print and develop the ultrasonically-powered MSNs, and the corresponding mechanism involving the oscillations of bubbles trapped in its inner cavity at the resonant frequency (Fig. 6A). Under an ultrasonic field, MSNs with three symmetric fins (of the same shape and uniformly placed) rotate counterclockwise, unlike the random motion of fins-free MNMs. When one of the fins is downsized to obtain the overall asymmetric structure, the MSNs present the nonlinear circular orbital motion (Fig. 6B). The MNMs with asymmetric fins could be propelled quickly under the acoustic field of 320 kHz and then by inserting the fins into the uroepithelium so as to immobilizing and slowly releasing drugs in the bladder of mice (Fig. 6C). However, unlike MNMs mentioned above, although they mentioned that the self-propulsion of MNMs contributes to the penetration of

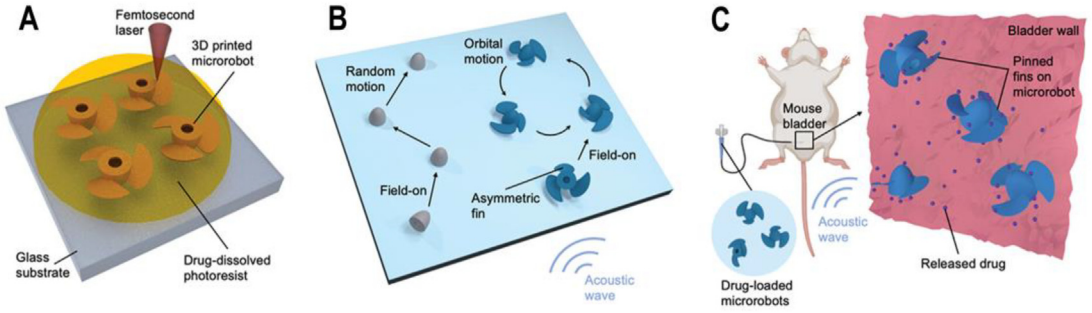

Figure 6 Schematic diagram of ultrasound-driven bubble-based micromotor. Schematic of (A) micromotor's 3D printing, (B) motion trajectory, and (C) the action mechanism of drug-loaded micromotors in the mouse bladder. Reprinted with the permission from Ref. 106. Copyright © 2021 American Chemical Society.

biological barriers, this work puts more emphasis on the ability of the motor with curved fins to immobilize itself to tissue matrices for slow drug release, which may be related to the fact that it has a larger size (20 μm) than other nanoscale MNMs which focus more on the penetration properties. In addition, *in vivo* effects need to be further evaluated.

5. Enhancement of adhesion, cell uptake and transport based on ligand−receptor interactions: Emphasis on targeting

Ligand-receptor interactions have garnered significant attention in the field of drug delivery due to their potential for active targeting/specific adhesion, penetration through physio-pathological barriers (*e.g.*, epithelial, tumor) and enhanced cellular uptake. Current targeting ligands mainly focus on receptors that are overexpressed on tumor cells or endothelial cells of the tumor vascular system (*e.g.*, vascular endothelial factor receptor, $\alpha_v\beta_3$ integrin)[107]. The latter target site may be more efficacious for intravenous administration of DDSs, so that the accumulation of DDSs in the tumor interstitial can be enhanced by the transcytosis-based *trans*-vascular transportation, thereby indirectly facilitating tumor cell internalization[108,109]. The specific penetration pattern of IDD, characterized by luminal-to-depth penetration, necessitates requires that IDDSs be designed to prioritize ligands corresponding to overexpressed receptors on the luminal side of the tumor tissue. Furthermore, functional ligands in IDDSs that combine the ability to target BC, promote permeation and internalization have received attention, and are summarized in Table 4[11,45,49,110-113].

In view of the specific interaction with easily internalized receptors overexpressed on the luminal surface of bladder tumor tissues and the surface of tumor cells, certain functional ligands such as folate[49], hyaluronic acid (HA)[110], transferrin[111], lectins[112], etc., have been proven to achieve targeted BC function while directly enhancing the tumor cellular uptake and tissue penetration of the drug carriers by activating the receptor-mediated endocytosis or transcytosis, thereby significantly improving antitumor effect. Notably, the corresponding receptors for some of these ligands (*e.g.*, WGA) are also expressed in normal uroepithelial cells, which is

Table 4 Functional ligands in IDDSs that can target bladder tumors and their mechanisms for promoting internalization/permeability.

Ligand	Functional receptor	Target cell line	System	Cargo	Internalization/ penetration mechanism	Ref.
R11	Unknown	T24	Self-Assembled R11-DNA NPs	DNA	Direct cell-to-cell transfer	45
Folate	Folate receptor	5637; HT1376; MBT2	Liposomes dispersed in the thermo-reversible hydrogel	Rap	Receptor-mediated endocytosis and transcytosis	49
HA	CD44	T24; 5637	Fluorescent probe-shielded polydopamine NPs	Dox	Clathrin-mediated endocytosis and transcytosis	110
Transferrin	Transferrin receptor	AY27	Liposome	$AlPcS_4$	Receptor-mediated endocytosis and transcytosis	111
WGA	Specific sugar motif	HT1376; 5637; SV-HUC-1	fBSA/WGA model conjugate	−	Receptor-mediated endocytosis and transcytosis	112,113
RGD	$\alpha_v\beta_3$ and $\alpha_v\beta_5$ integrins	T24	Glutathione-responsive prodrug NPs	PTX−SS−HPPH; Platinum nanozyme	Receptor-mediated endocytosis and transcytosis	11

−, not applicable.
Rap, rapamycin; HA, hyaluronic acid; $AlPcS_4$, aluminum phthalocyanine tetrasulfonat; fBSA, fluorescein-labeled bovine serum albumin; WGA, wheat germ agglutinin; RGD, peptide Arg-Gly-Asp; PTX, paclitaxel; HPPH, 2-(1-hexyloxyethyl)-2-devinyl pyropheophorbidea; Dox, doxorubicin; NPs, nanoparticles.

why Brauner et al.[114] grafted WGA as the functional ligand to enhance uroepithelial-specific adhesion onto the surface of drug-loaded PLGA NPs, enabling effective intravesical treatment of urinary tract infections. However, due to the differential expression of the corresponding receptors in normal and diseased tissues, WGA remains one of the BC-targeted ligands[115]. Therefore, careful consideration should be given to the heterogeneity of target sites across specific disease states when selecting functional ligands.

Unlike the targeted ligands mentioned above, which are based on transcytosis activation to promote permeation, other ligands can also enhance delivery efficiency by modulating other internalized, transport pathways of DDS. Based on the ability to target bladder tumors and its positive charge characteristics, R11 (one of the cell-penetrating peptides) has been used as the carrier for gene delivery to treat bladder cancer[116,117]. Zhang et al.[45] utilized the electrostatic interaction between R11 and therapeutic DNA to prepare R11-DNA nanocomplexes and used free R11 pretreatment to prevent the negatively charged GAG layer and tumor cell membranes from destabilizing the nanocomplexes. Exploration of the permeation mechanism showed that the combination of R11 with DNA changed the entry mode of these two components into the cells, from clathrin-mediated endocytosis to clathrin-independent endocytosis, while enhancing the cellular uptake and lysosomal escape of the DNA, thereby facilitating intracellular transport of DNA to the nucleus. In addition, the R11 modification promotes the transport of DNA to other cells by a direct transfer mechanism without going through the extracellular matrix.

An example closely related to the clinical intravesical treatment of bladder cancer targets the surgical bed environment after TURBT, where microtumors may remain, and focus on bioadhesion functions based on ligand−receptor interactions. Inspired by fibronectin (FN)-binding peptide-mediated bacterial adhesion to wounds, Wang et al.[76] developed a peptide (BTN)-based self-assembling and Dox-loaded transformable nanoparticle. BTN peptides consisting of FN-binding peptides (targeting and adhesion), KLVFF peptides (binding with hydrogen-bonded/hydrophilic), and dodecyl chains (hydrophobic) self-assembled to form nanoparticles in which Dox was loaded in its hydrophobic structural domain. Led by the FN-binding peptide motifs in the BTN, Dox@BTN selectively adhered to the surgical wound, while the interaction with FNs at the wound site broke the hydrophobic−hydrophilic equilibrium of those self-assembled nanoparticles and triggered the intermolecular hydrogen-bonding interactions among the KLVFF motifs, thereby realizing the change from particles to fibers and forming the 3D fibrous network that covered the surgical wound. In the tumor partially resected mouse model, the residual tumor inhibitory capacity of Dox@BTN (mean tumor volume of 100.7 nm^3) outperformed that of the control group (553.5 nm^3), the perfused Dox alone (257.1 nm^3), or the BGC group (384.7 nm^3). However, this surgical wound-based targeting and adherent IDDSs was limited by the pre-screening of the surgery for tumor sites.

6. Switching between adhesion and penetration: Dual encapsulation and size/charge transformable systems

Trying to achieve both adhesion and permeation functions on a single carrier is to some extent contradictory, as adhesion to the bladder mucus layer while leaving DDSs on the surface is detrimental to permeation, and *vice versa*. Dual encapsulation systems refer to the encapsulation of small particles into larger carriers and allow sequential switching between the two for different functions, resulting in better control of drug retention, penetration and release[118].

In applications of IDD, the most common form of dual encapsulation systems is the combination of *in situ* formed gels and nanoparticles. Usually, the *in situ* gel acts as the reservoir for the sustained release of nanoparticles on bladder mucosa, compensating for its deficiency of adhesion. On the other hand, nanoparticles are designed for mucus penetration, targeting, and enhancing hydrophobic drug solubility and so on. For example, HA-coated iron oxide nanoparticles (IONPs) were encapsulated into the gel platform synthesized from PAMAM and aldehyde hyaluronic acid, aiming to overcome the physiological barrier of the bladder for effective drug delivery to bladder tumor (Fig. 7A)[119]. The targeting and adhesion of the gel platform to the BC surface derives from the chemical anchoring of the aldehyde functional group to collagen expressed abundantly in the tumor extracellular matrix. After sustainable release on the tumor surface, HA-IONP penetrates the tumor tissue by thermal ablation under near-infrared light, subsequently targeting and interacting with CD44 overexpressed in BC cell membranes guided by HA, thereby enhancing cellular uptake and exerting iron death-based antitumor effects. In the *in situ* bladder cancer mouse model, this stepwise intravesical delivery system resulted in a 10-fold higher accumulation of IONP in tumor tissues than intravenous injection. Furthermore, other combinatorial forms such as microparticles-nanoparticles[120,121] and nanoparticles-nanoparticles[122] have been used for the construction of dual-encapsulation systems, which conquer mucus and tissue barriers through the intelligent sequential switching of different functions (especially adhesion to permeation).

On the other hand, based on the effects of electrostatic adsorption and size exclusion on the mucus trapping ability, the switching between adhesion and permeation functions can also be realized by the transformation of charge or size of DDSs. Le-Vinh et al.[123] recently reported a solid lipid nanosystem (SLN) that can be triggered by alkaline phosphatase (AP) to switch from nanometer to micrometer size. Negatively charged phospholipid surfactants were modified on the surface of SLNs loaded with octadecylamine to avoid electrostatic adsorption and promote mucus penetration. AP-triggered phosphate removal and subsequent exposure of positively charged octadecylamine residues contributed to the aggregation of SLNs and size increase (Fig. 7B). When penetrating the mucus and approaching the epithelial cell absorbing membrane, the size transform of SLNs is triggered by APs so that SLNs with microscale size can act as the drug reservoir for sustained drug release at this site and avoid the possibility of their reverse diffusion into the external zone of the mucus (back the way they came). Similar mechanistic advantages have also been demonstrated in polyethylene imine-6-phosphogluconic acid nanoparticles[124] and phosphorylated chitosan-stearic acid conjugates micelles[125] which are used for transmucosal delivery in the digestive tract, but such permeation-adhesion switching strategies based on charge or size transformation have not yet been investigated for IDD.

7. Summary and prospects

IDD has shown significant advantages in the pharmacological treatment of bladder diseases (especially BC), improving efficacy while avoiding systemic off-target side effects. However, the

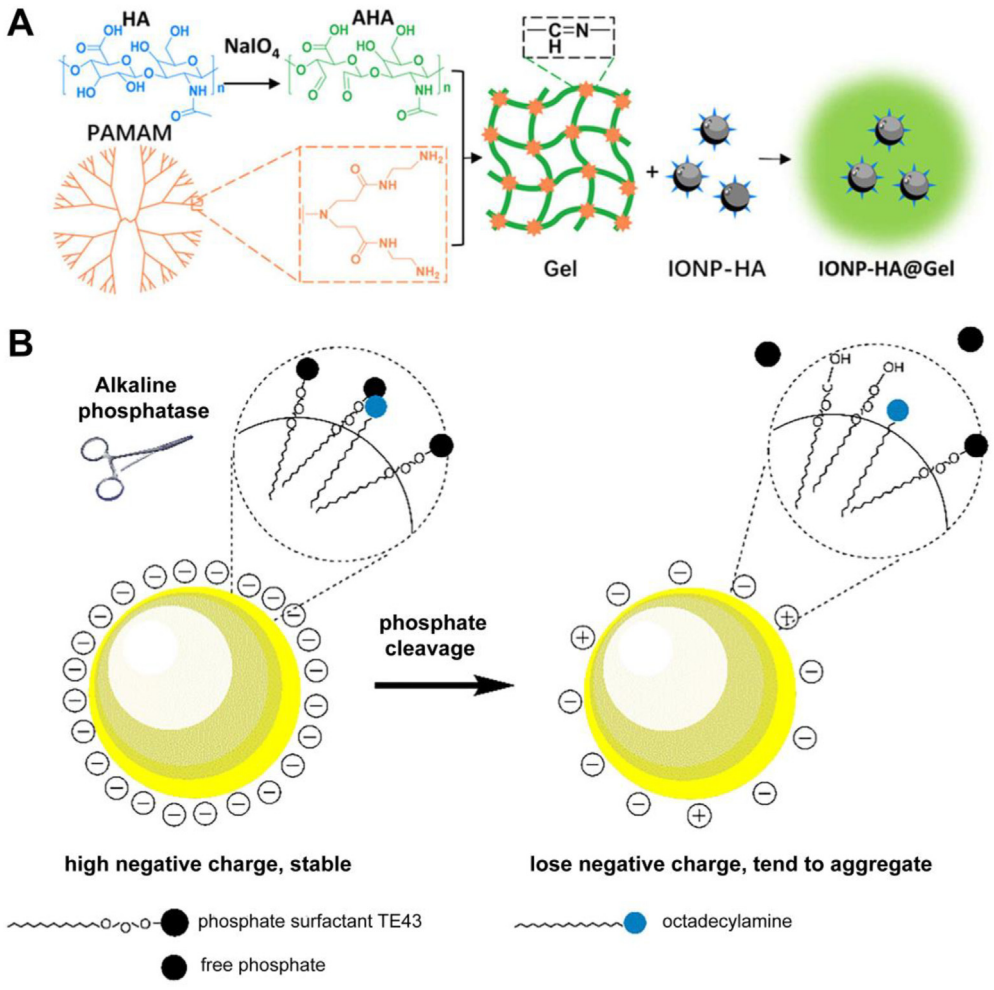

Figure 7 DDSs with the ability to transform between functions. (A) Schematic diagram of the preparation process of a dual encapsulation system in the form of nanoparticles in gel. Reprinted with the permission from Ref. 120. Copyright © 2021 American Chemical Society. (B) The mechanism of size/charge transformable system triggered by alkaline phosphatase. Reprinted with the permission from Ref. 124.

physiological barriers of the bladder (urine and periodic urination, mucus layer, and uroepithelial/solid tumor tissues) severely impede effective drug delivery to the target site located deep in the bladder, and there is an urgent need for the development of IDDSs based on a thorough understanding of the bladder pathophysiology. Premature clearance of DDSs can be avoided by creating drug reservoirs in different parts of the bladder (floating in urine, adhering to the bladder lining, and lodging in tumor cells). To enhance bladder permeability, different strategies have been implemented, such as the incorporation of mucus-inert coatings, TJs modulators, photothermal particles, mucolytic enzymes, etc. in the formulations, as well as the construction of self-propelled micro/nano-motors. Thanks to ligand—receptor interactions and the subsequent transport activated by them (*e.g.*, transcytosis and direct cell-to-cell transfer), ligand components such as HA, R11, etc., have been used to confer targeting to DDSs while enhancing their adhesion and permeability. In addition, dual encapsulation and size/charge transform strategies have the potential to meet the conflicting requirements needed for IDDSs to overcome different barriers in the IDD process, as they enable inter-switching between different functions (especially adhesion and permeation).

Given the special complexity of bladder physiology, studies need to pay close attention to the scientific soundness of drug carrier design. First, carrier materials, especially for the construction of adherent DDSs, need to be focused on their biocompatibility, *in vivo* degradation properties and interaction with urine/mucus. Inadequate degradation products and possible gel clumps due to interaction with urine/mucus may obstruct, irritate the urinary tract and thus affect physiological function. Second, the selection and assembly of surface modifying groups/targeting ligands should fully consider the characteristics of the bladder physiological barrier, the heterogeneity of the disease or tumor, and the target of drug action. High affinity, stability, and effectiveness are key evaluation indicators. Third, IDDSs capable of switching between functions are important for overcoming the different barriers encountered in IDD, but the "smartness" of switching, *i.e.*, specificity and timing, remains a limiting factor for effective treatment. Therefore, it is necessary to fully and correctly understand the physiological characteristics and disease mechanisms of the bladder, and accordingly design and construct IDDSs with appropriate materials, which requires the joint efforts of clinical experts and Formulation researchers. It is believed that the development of safer and more effective IDDSs and their

subsequent application in the clinic will bring good news for many bladder disease patients (especially BC patients).

Acknowledgments

This review was supported by Shanghai Xuhui medical research project (SHXH202110 and SHXH202230, China), the Natural Science Foundation of Shanghai (21ZR1447900, China) and Key Discipline Construction Project (SHXHZDXK202310, China) of Shanghai Xuhui Health System.

Author contributions

Zheng-an Li: Conceptualization, Visualization, Writing − original draft. Kai-chao Wen: Formal analysis. Ji-heng Liu: Formal analysis. Chuan Zhang: Supervision. Feng Zhang: Supervision. Feng-qian Li: Conceptualization, Resources, Supervision, Writing − review & editing.

Conflicts of interest

There are no conflicts to declare.

References

1. Sharma S, Basu B. Biomaterials assisted reconstructive urology: the pursuit of an implantable bioengineered neo-urinary bladder. *Biomaterials* 2022;**281**:121331.
2. Palugan L, Cerea M, Cirilli M, Moutaharrik S, Maroni A, Zema L, et al. Intravesical drug delivery approaches for improved therapy of urinary bladder diseases. *Int J Pharm X* 2021;**3**:100100.
3. Jubber I, Ong S, Bukavina L, Black PC, Compérat E, Kamat AM, et al. Epidemiology of bladder cancer in 2023: a systematic review of risk factors. *Eur Urol* 2023;**84**:176−90.
4. Seidl C. Targets for therapy of bladder cancer. *Semin Nucl Med* 2020; **50**:162−70.
5. Tang C, Liu H, Fan YP, He JH, Li FQ, Wang J, et al. Functional nanomedicines for targeted therapy of bladder cancer. *Front Pharmacol* 2021;**12**:778973.
6. Jain P, Kathuria H, Momin M. Clinical therapies and nano drug delivery systems for urinary bladder cancer. *Pharmacol Ther* 2021; **226**:107871.
7. Naeye B, Deschout H, Caveliers V, Descamps B, Braeckmans K, Vanhove C, et al. *In vivo* disassembly of IV administered siRNA matrix nanoparticles at the renal filtration barrier. *Biomaterials* 2013; **34**:2350−8.
8. Hu J, Chen JB, Ou ZY, Chen HG, Liu Z, Chen MF, et al. Neoadjuvant immunotherapy, chemotherapy, and combination therapy in muscle-invasive bladder cancer: a multi-center real-world retrospective study. *Cell Rep Med* 2022;**3**:100785.
9. Babjuk M, Burger M, Compérat EM, Gontero P, Mostafid AH, Palou J, et al. European association of urology guidelines on non-muscle-invasive bladder cancer (TaT1 and carcinoma *in situ*) —2019 update. *Eur Urol* 2019;**76**:639−57.
10. Cheong JKK, Ooi EH, Chiew YS, Menichetti L, Armanetti P, Franchini MC, et al. Gold nanorods assisted photothermal therapy of bladder cancer in mice: a computational study on the effects of gold nanorods distribution at the centre, periphery, and surface of bladder cancer. *Comput Methods Programs Biomed* 2023;**230**:107363.
11. Hao Y, Chen YW, He XL, Han RX, Yang CL, Liu TL, et al. RGD peptide modified platinum nanozyme co-loaded glutathione-responsive prodrug nanoparticles for enhanced chemo-photodynamic bladder cancer therapy. *Biomaterials* 2023;**293**:121975.
12. Qi FG, Bao QQ, Hu P, Guo YD, Yan Y, Yao XD, et al. Mild magnetic hyperthermia-activated immuno-responses for primary bladder cancer therapy. *Biomaterials* 2024;**307**:122514.
13. GuhaSarkar S, Banerjee R. Intravesical drug delivery: challenges, current status, opportunities and novel strategies. *J Control Release* 2010;**148**:147−59.
14. Au JL, Badalament RA, Wientjes MG, Young DC, Warner JA, Venema PL, et al. Methods to improve efficacy of intravesical mitomycin C: results of a randomized phase III trial. *J Natl Cancer Inst* 2001;**93**:597−604.
15. Tyagi P, Kashyap M, Hensley H, Yoshimura N. Advances in intravesical therapy for urinary tract disorders. *Expert Opin Drug Deliv* 2016;**13**:71−84.
16. Gao X, Au JL, Badalament RA, Wientjes MG. Bladder tissue uptake of mitomycin C during intravesical therapy is linear with drug concentration in urine. *Clin Cancer Res* 1998;**4**:139−43.
17. Balhara N, Devi M, Balda A, Phour M, Giri A. Urine; a new promising biological fluid to act as a non-invasive biomarker for different human diseases. *Urine* 2023;**5**:40−52.
18. GuhaSarkar S, More P, Banerjee R. Urothelium-adherent, ion-triggered liposome-in-gel system as a platform for intravesical drug delivery. *J Control Release* 2017;**245**:147−56.
19. Hortelão AC, Patiño T, Perez-Jiménez A, Blanco À, Sánchez S. Enzyme-powered nanobots enhance anticancer drug delivery. *Adv Funct Mater* 2018;**28**:1705086.
20. Simó C, Serra-Casablancas M, Hortelao AC, Di Carlo V, Guallar-Garrido S, Plaza-García S, et al. Urease-powered nanobots for radionuclide bladder cancer therapy. *Nat Nanotechnol* 2024;**19**: 554−64.
21. Ayres JW, Weidler DJ, MacKichan J, Wagner JG. Circadian rhythm of urinary pH in man with and without chronic antacid administration. *Eur J Clin Pharmacol* 1977;**12**:415−20.
22. Kang MR, Yang G, Place RF, Charisse K, Epstein-Barash H, Manoharan M, et al. Intravesical delivery of small activating RNA formulated into lipid nanoparticles inhibits orthotopic bladder tumor growth. *Cancer Res* 2012;**72**:5069−79.
23. Kong N, Zhang RN, Wu GW, Sui XB, Wang JQ, Kim NY, et al. Intravesical delivery of KDM6A-mRNA *via* mucoadhesive nanoparticles inhibits the metastasis of bladder cancer. *Proc Natl Acad Sci U S A* 2022;**119**:e2112696119.
24. Thongboonkerd V, Mungdee S, Chiangjong W. Should urine pH be adjusted prior to gel-based proteome analysis?. *J Proteome Res* 2009; **8**:3206−11.
25. N'Dow J, Jordan N, Robson CN, Neal DE, Pearson JP. The bladder does not appear to have a dynamic secreted continuous mucous gel layer. *J Urol* 2005;**173**:2025−31.
26. Cornish J, Nickel JC, Vanderwee M, Costerton JW. Ultrastructural visualization of human bladder mucous. *Urol Res* 1990;**18**:263−6.
27. Parsons CL, Greenspan C, Moore SW, Mulholland SG. Role of surface mucin in primary antibacterial defense of bladder. *Urology* 1977;**9**:48−52.
28. Bassi PF, Costantini E, Foley S, Palea S. Glycosaminoglycan therapy for bladder diseases: emerging new treatments. *Eur Urol Suppl* 2011; **10**:451−9.
29. Dalghi MG, Montalbetti N, Carattino MD, Apodaca G. The urothelium: life in a liquid environment. *Physiol Rev* 2020;**100**:1621−705.
30. Murgia X, Loretz B, Hartwig O, Hittinger M, Lehr CM. The role of mucus on drug transport and its potential to affect therapeutic outcomes. *Adv Drug Deliv Rev* 2018;**124**:82−97.
31. Poinard B, Lam SAE, Neoh KG, Kah JCY. Mucopenetration and biocompatibility of polydopamine surfaces for delivery in an *ex vivo* porcine bladder. *J Control Release* 2019;**300**:161−73.
32. Zhang P, Wu GQ, Zhang DH, Lai WF. Mechanisms and strategies to enhance penetration during intravesical drug therapy for bladder cancer. *J Control Release* 2023;**354**:69−79.
33. Liu FQ, Guo C, Li XD, Li YM, Xu SY, James TD, et al. A versatile nano-transformer for efficient localization-specific imaging and synergistic therapy of bladder cancer. *Nano Today* 2024;**54**:102116.

34. de Lima CSA, Rial-Hermida MI, de Freitas LF, Pereira-da-Mota AF, Vivero-Lopez M, Ferreira AH, et al. Mucoadhesive gellan gum-based and carboxymethyl cellulose-based hydrogels containing gemcitabine and papain for bladder cancer treatment. *Int J Biol Macromol* 2023;**242**:124957.
35. Amiri Z, Hasani A, Abedini F, Malek M, Madaah Hosseini HR. Urease-powered black TiO_2 micromotors for photothermal therapy of bladder cancer. *ACS Appl Mater* 2024;**16**:3019−30.
36. Wilczak M, Surman M, Przybyło M. Altered glycosylation in progression and management of bladder cancer. *Molecules* 2023;**28**:3436.
37. De Klerk DP. The glycosaminoglycans of human bladder cancers of varying grade and stage. *J Urol* 1985;**134**:978−81.
38. Janssen D, Jansen K, Schalken J, Heesakkers J. 824 sulphated glycosaminoglycans a space key (GAG's) contribute to the bladder barrier. *J Urol* 2012;**187**:e336−7.
39. Kobayashi T, Owczarek TB, McKiernan JM, Abate-Shen C. Modelling bladder cancer in mice: opportunities and challenges. *Nat Rev Cancer* 2015;**15**:42−54.
40. Lewis SA. Everything you wanted to know about the bladder epithelium but were afraid to ask. *Am J Physiol Ren Physiol* 2000;**278**:F867−74.
41. Haynes MD, Martin TA, Jenkins SA, Kynaston HG, Matthews PN, Jiang WG. Tight junctions and bladder cancer (review). *Int J Mol Med* 2005;**16**:3−9.
42. Brunner J, Ragupathy S, Borchard G. Target specific tight junction modulators. *Adv Drug Deliv Rev* 2021;**171**:266−88.
43. Sun XL, Song XH, Guo P, Zhang D, Zuo SH, Leng K, et al. Improvement of the bladder perfusion curative effect through tight junction protein degradation induced by magnetic temperature-sensitive hydrogels. *Front Bioeng Biotechnol* 2022;**10**:958072.
44. Guo L, Zhang Y, Yang ZP, Peng H, Wei RX, Wang CF, et al. Tunneling nanotubular expressways for ultrafast and accurate M1 macrophage delivery of anticancer drugs to metastatic ovarian carcinoma. *ACS Nano* 2019;**13**:1078−96.
45. Zhang P, Zhang HB, Zheng B, Wang H, Qi XL, Wang S, et al. Combined self-assembled hendeca-arginine nanocarriers for effective targeted gene delivery to bladder cancer. *Int J Nanomedicine* 2022;**17**:4433−48.
46. Tschernig T. Connexins and gap junctions in cancer of the urinary tract. *Cancers (Basel)* 2019;**11**:704.
47. Wang YF, Shen ZF, Xiang FY, Wang H, Zhang P, Zhang Q. The direct transfer approach for transcellular drug delivery. *Drug Deliv* 2023;**30**:2288799.
48. Chen SQ, Zhou Q, Wang GW, Zhou ZX, Tang JB, Xie T, et al. Effect of cationic charge density on transcytosis of polyethylenimine. *Biomacromolecules* 2021;**22**:5139−50.
49. Yoon HY, Chang IH, Goo YT, Kim CH, Kang TH, Kim SY, et al. Intravesical delivery of rapamycin *via* folate-modified liposomes dispersed in thermo-reversible hydrogel. *Int J Nanomedicine* 2019;**14**:6249−68.
50. Kou LF, Sun J, Zhai YL, He ZG. The endocytosis and intracellular fate of nanomedicines: implication for rational design. *Asian J Pharm Sci* 2013;**8**:1−10.
51. Chen NX, He Y, Zang MM, Zhang YX, Lu HY, Zhao QF, et al. Approaches and materials for endocytosis-independent intracellular delivery of proteins. *Biomaterials* 2022;**286**:121567.
52. Jing WQ, Chen C, Wang GY, Han MS, Chen SZ, Jiang X, et al. Metabolic modulation of intracellular ammonia *via* intravesical instillation of nanoporter-encased hydrogel eradicates bladder carcinoma. *Adv Sci (Weinh)* 2023;**10**:e2206893.
53. Lin TS, Wu JH, Zhao XZ, Lian HB, Yuan AH, Tang XL, et al. *In situ* floating hydrogel for intravesical delivery of adriamycin without blocking urinary tract. *J Pharm Sci* 2014;**103**:927−36.
54. Lin TS, Zhang YF, Wu JH, Zhao XZ, Lian HB, Wang W, et al. A floating hydrogel system capable of generating CO_2 bubbles to diminish urinary obstruction after intravesical instillation. *Pharm Res* 2014;**31**:2655−63.
55. Zhu GC, Zhang YF, Wang KK, Zhao XZ, Lian HB, Wang W, et al. Visualized intravesical floating hydrogel encapsulating vaporized perfluoropentane for controlled drug release. *Drug Deliv* 2016;**23**:2820−6.
56. Lin TS, Zhao XZ, Zhang YF, Lian HB, Zhuang JL, Zhang Q, et al. Floating hydrogel with self-generating micro-bubbles for intravesical instillation. *Materials (Basel)* 2016;**9**:1005.
57. Deng QR, Xie JY, Kong SY, Tang TM, Zhou JH. Long-term retention microbubbles with three-layer structure for floating intravesical instillation delivery. *Small* 2023;**19**:e2205630.
58. Liu C, Su MY, Xu ZB, Huang X. Multi-layered powder-in-hydrogel capsules by magnetism-assisted bubbling method. *Mater Lett* 2022;**318**:132144.
59. Fu K, Zhou YF, Hou J, Shi T, Ni J, Li X, et al. Floating poly(lactic-*co*-glycolic acid)-based controlled-release drug delivery system for intravesical instillation. *J Int Med Res* 2023;**51**:3000605231162065.
60. Netsomboon K, Bernkop-Schnürch A. Mucoadhesive *vs.* mucopenetrating particulate drug delivery. *Eur J Pharm Biopharm* 2016;**98**:76−89.
61. Ali MS, Metwally AA, Fahmy RH, Osman R. Chitosan-coated nanodiamonds: mucoadhesive platform for intravesical delivery of doxorubicin. *Carbohydr Polym* 2020;**245**:116528.
62. Wang BW, Zhang KB, Wang JD, Zhao RB, Zhang Q, Kong XD. Poly(amidoamine)-modified mesoporous silica nanoparticles as a mucoadhesive drug delivery system for potential bladder cancer therapy. *Colloids Surf B Biointerfaces* 2020;**189**:110832.
63. Chen CC, Fa YC, Kuo YY, Liu YC, Lin CY, Wang XH, et al. Thiolated mesoporous silica nanoparticles as an immunoadjuvant to enhance efficacy of intravesical chemotherapy for bladder cancer. *Adv Sci (Weinh)* 2023;**10**:e2204643.
64. Anzengruber M, Wimmer L, Szuchar R, Skoll K, Wirth M, Gabor F. Log*P* of *N*-acyl-gemcitabine and lectin-corona emerge as key parameters in nanoparticulate intravesical cancer therapy. *Eur J Pharm Sci* 2023;**180**:106330.
65. Wang LL, Qi F, Bi LP, Yan J, Han XQ, Wang YJ, et al. Targeted hollow pollen silica nanoparticles for enhanced intravesical therapy of bladder cancer. *Biomater Sci* 2023;**11**:4948−59.
66. Kaldybekov DB, Filippov SK, Radulescu A, Khutoryanskiy VV. Maleimide-functionalised PLGA-PEG nanoparticles as mucoadhesive carriers for intravesical drug delivery. *Eur J Pharm Biopharm* 2019;**143**:24−34.
67. Sahatsapan N, Rojanarata T, Ngawhirunpat T, Opanasopit P, Patrojanasophon P. Doxorubicin-loaded chitosan-alginate nanoparticles with dual mucoadhesive functionalities for intravesical chemotherapy. *J Drug Deliv Sci Technol* 2021;**63**:102481.
68. Kolawole OM, Lau WM, Khutoryanskiy VV. Methacrylated chitosan as a polymer with enhanced mucoadhesive properties for transmucosal drug delivery. *Int J Pharm* 2018;**550**:123−9.
69. Lehr CM. Lectin-mediated drug delivery: the second generation of bioadhesives. *J Control Release* 2000;**65**:19−29.
70. Li H, Dong WF, Zhou JY, Xu XM, Li FQ. Triggering effect of *N*-acetylglucosamine on retarded drug release from a lectin-anchored chitosan nanoparticles-in-microparticles system. *Int J Pharm* 2013;**449**:37−43.
71. Ward GK, Stewart SS, Price GB, Mackillop WJ. Cellular heterogeneity in normal human urothelium: quantitative studies of lectin binding. *Histochem J* 1987;**19**:337−44.
72. Wu X, Wei YB, Lin RC, Chen PZ, Hong ZW, Zeng R, et al. Multi-responsive mesoporous polydopamine composite nanorods cooperate with nano-enzyme and photosensitiser for intensive immunotherapy of bladder cancer. *Immunology* 2022;**167**:247−62.
73. Huo F, Zhang Y, Li YR, Bu HG, Zhang YL, Li W, et al. Mannose-targeting concanavalin A-epirubicin conjugate for targeted intravesical chemotherapy of bladder cancer. *Chem Asian J* 2022;**17**:e202200342.
74. Bernkop-Schnürch A, Kast CE, Guggi D. Permeation enhancing polymers in oral delivery of hydrophilic macromolecules: thiomer/GSH systems. *J Control Release* 2003;**93**:95−103.

75. Liu J, Yang TY, Dai LQ, Shi K, Hao Y, Chu BY, et al. Intravesical chemotherapy synergize with an immune adjuvant by a thermosensitive hydrogel system for bladder cancer. *Bioact Mater* 2024;**31**:315−32.
76. Wang JQ, Yang PP, Hou DY, Yan YQ, Yue K, Zhong WS, et al. Bacteria-inspired transformable nanoparticle targets and covers residual tumor against bladder cancer recurrence. *Nano Today* 2022;**45**:101551.
77. Sun YP, Sha YJ, Cui GH, Meng FH, Zhong ZY. Lysosomal-mediated drug release and activation for cancer therapy and immunotherapy. *Adv Drug Deliv Rev* 2023;**192**:114624.
78. Zeng S, Ou HL, Gao ZY, Zhang JT, Li C, Liu Q, et al. HCPT-peptide prodrug with tumor microenvironment-responsive morphology transformable characteristic for boosted bladder tumor chemotherapy. *J Control Release* 2021;**330**:715−25.
79. Hou DY, Zhang NY, Wang MD, Xu SX, Wang ZJ, Hu XJ, et al. *In situ* constructed nano-drug depots through intracellular hydrolytic condensation for chemotherapy of bladder cancer. *Angew Chem Int Ed Engl* 2022;**61**:e202116893.
80. Witten J, Samad T, Ribbeck K. Selective permeability of mucus barriers. *Curr Opin Biotechnol* 2018;**52**:124−33.
81. Wang YY, Lai SK, Suk JS, Pace A, Cone R, Hanes J. Addressing the PEG mucoadhesivity paradox to engineer nanoparticles that "slip" through the human mucus barrier. *Angew Chem Int Ed Engl* 2008;**47**:9726−9.
82. Li QS, Wen CY, Yang J, Zhou XC, Zhu YN, Zheng J, et al. Zwitterionic biomaterials. *Chem Rev* 2022;**122**:17073−154.
83. Pereira de Sousa I, Steiner C, Schmutzler M, Wilcox MD, Veldhuis GJ, Pearson JP, et al. Mucus permeating carriers: formulation and characterization of highly densely charged nanoparticles. *Eur J Pharm Biopharm* 2015;**97**:273−9.
84. Khutoryanskiy VV. Beyond PEGylation: alternative surface-modification of nanoparticles with mucus-inert biomaterials. *Adv Drug Deliv Rev* 2018;**124**:140−9.
85. Li LD, Crouzier T, Sarkar A, Dunphy L, Han J, Ribbeck K. Spatial configuration and composition of charge modulates transport into a mucin hydrogel barrier. *Biophys J* 2013;**105**:1357−65.
86. Li GZ, Lei QF, Wang F, Deng DS, Wang SP, Tian LL, et al. Fluorinated polymer mediated transmucosal peptide delivery for intravesical instillation therapy of bladder cancer. *Small* 2019;**15**:e1900936.
87. Li GZ, Yuan SM, Deng DS, Ou T, Li YQ, Sun R, et al. Fluorinated polyethylenimine to enable transmucosal delivery of photosensitizer-conjugated catalase for photodynamic therapy of orthotopic bladder tumors postintravesical instillation. *Adv Funct Mater* 2019;**29**:1901932.
88. Cheng X, Zeng XL, Zheng Y, Wang X, Tang RP. Surface-fluorinated and pH-sensitive carboxymethyl chitosan nanoparticles to overcome biological barriers for improved drug delivery *in vivo*. *Carbohydr Polym* 2019;**208**:59−69.
89. Li GZ, Wang SP, Deng DS, Xiao ZS, Dong ZL, Wang ZP, et al. Fluorinated chitosan to enhance transmucosal delivery of sonosensitizer-conjugated catalase for sonodynamic bladder cancer treatment post-intravesical instillation. *ACS Nano* 2020;**14**:1586−99.
90. Tan WS, Kelly JD. Intravesical device-assisted therapies for non-muscle-invasive bladder cancer. *Nat Rev Urol* 2018;**15**:667−85.
91. Sun ZD, Zhang WY, Ye ZC, Yuan L, Fu ML, Liu XM, et al. NIR-II-triggered doxorubicin release for orthotopic bladder cancer chemo-photothermal therapy. *Nanoscale* 2022;**14**:17929−39.
92. Yang XP, Su LJ, La Rosa FG, Smith EE, Schlaepfer IR, Cho SK, et al. The antineoplastic activity of photothermal ablative therapy with targeted gold nanorods in an orthotopic urinary bladder cancer model. *Bladder Cancer* 2017;**3**:201−10.
93. Zhan YL, Wen KC, Li ZA, Sun P, Li FQ. Dielectric and magnetic composites of Fe_3O_4@APNs for superior microwave thermal effect. *ACS Biomater Sci Eng* 2024;**10**:791−9.
94. Menzel C, Bernkop-Schnürch A. Enzyme decorated drug carriers: targeted swords to cleave and overcome the mucus barrier. *Adv Drug Deliv Rev* 2018;**124**:164−74.
95. Suk JS, Boylan NJ, Trehan K, Tang BC, Schneider CS, Lin JM, et al. *N*-Acetylcysteine enhances cystic fibrosis sputum penetration and airway gene transfer by highly compacted DNA nanoparticles. *Mol Ther* 2011;**19**:1981−9.
96. Ramirez-Velez I, Belardi B. Storming the gate: new approaches for targeting the dynamic tight junction for improved drug delivery. *Adv Drug Deliv Rev* 2023;**199**:114905.
97. Yu C, Wang S, Lai WF, Zhang DH. The progress of chitosan-based nanoparticles for intravesical bladder cancer treatment. *Pharmaceutics* 2023;**15**:211.
98. Li G, He SS, Schätzlein AG, Weiss RM, Martin DT, Uchegbu IF. Achieving highly efficient gene transfer to the bladder by increasing the molecular weight of polymer-based nanoparticles. *J Control Release* 2021;**332**:210−24.
99. Tian H, Ou JQ, Wang Y, Sun J, Gao JB, Ye YC, et al. Bladder microenvironment actuated proteomotors with ammonia amplification for enhanced cancer treatment. *Acta Pharm Sin B* 2023;**13**:3862−75.
100. Hortelão AC, Carrascosa R, Murillo-Cremaes N, Patiño T, Sánchez S. Targeting 3D bladder cancer spheroids with urease-powered nanomotors. *ACS Nano* 2019;**13**:429−39.
101. Choi H, Cho SH, Hahn SK. Urease-powered polydopamine nanomotors for intravesical therapy of bladder diseases. *ACS Nano* 2020;**14**:6683−92.
102. Tang SS, Zhang FY, Gong H, Wei FN, Zhuang J, Karshalev E, et al. Enzyme-powered Janus platelet cell robots for active and targeted drug delivery. *Sci Robot* 2020;**5**:eaba6137.
103. Cong ZQ, Tang SS, Xie LM, Yang M, Li YY, Lu DD, et al. Magnetic-powered janus cell robots loaded with oncolytic adenovirus for active and targeted virotherapy of bladder cancer. *Adv Mater* 2022;**34**:e2201042.
104. Lee JG, Raj RR, Thome CP, Day NB, Martinez P, Bottenus N, et al. Bubble-based microrobots with rapid circular motions for epithelial pinning and drug delivery. *Small* 2023;**19**:e2300409.
105. Sun R, Liu XC, Li GZ, Wang H, Luo YX, Huang GX, et al. Photoactivated H_2 nanogenerator for enhanced chemotherapy of bladder cancer. *ACS Nano* 2020;**14**:8135−48.
106. Hortelao AC, Simó C, Guix M, Guallar-Garrido S, Julián E, Vilela D, et al. Swarming behavior and *in vivo* monitoring of enzymatic nanomotors within the bladder. *Sci Robot* 2021;**6**:eabd2823.
107. Lin GY, Zhang MQ. Ligand chemistry in antitumor theranostic nanoparticles. *Acc Chem Res* 2023;**56**:1578−90.
108. Kutoka PT, Seidu TA, Baye V, Khamis AM, Omonova CTq, Wang B. Insights into tumor microenvironment (TME) and the nano approaches to suppress tumor growth. *OpenNano* 2022;**7**:100041.
109. Wang XW, Qiu YH, Wang MY, Zhang CH, Zhang TS, Zhou HM, et al. Endocytosis and organelle targeting of nanomedicines in cancer therapy. *Int J Nanomedicine* 2020;**15**:9447−67.
110. Qiu HP, Wang JW, Zhi Y, Yan BH, Huang YD, Li JJ, et al. Hyaluronic acid-conjugated fluorescent probe-shielded polydopamine nanomedicines for targeted imaging and chemotherapy of bladder cancer. *ACS Appl Mater Inter* 2023;**15**:46668−80.
111. Derycke AS, Kamuhabwa A, Gijsens A, Roskams T, De Vos D, Kasran A, et al. Transferrin-conjugated liposome targeting of photosensitizer $AlPcS_4$ to rat bladder carcinoma cells. *J Natl Cancer Inst* 2004;**96**:1620−30.
112. Neutsch L, Eggenreich B, Herwig E, Marchetti-Deschmann M, Allmaier G, Gabor F, et al. Lectin bioconjugates trigger urothelial cytoinvasion—a glycotargeted approach for improved intravesical drug delivery. *Eur J Pharm Biopharm* 2012;**82**:367−75.
113. Neutsch L, Eggenreich B, Herwig E, Marchetti-Deschmann M, Allmaier G, Gabor F, et al. Biomimetic delivery strategies at the urothelium: targeted cytoinvasion in bladder cancer cells *via* lectin bioconjugates. *Pharm Res* 2014;**31**:819−32.

114. Brauner B, Semmler J, Rauch D, Nokaj M, Haiss P, Schwarz P, et al. Trimethoprim-loaded PLGA nanoparticles grafted with WGA as potential intravesical therapy of urinary tract infections—studies on adhesion to SV-HUCs under varying time, pH, and drug-loading conditions. *ACS Omega* 2020;**5**:17377−84.
115. Apfelthaler C, Skoll K, Ciola R, Gabor F, Wirth M. A doxorubicin loaded colloidal delivery system for the intravesical therapy of non-muscle invasive bladder cancer using wheat germ agglutinin as targeter. *Eur J Pharm Biopharm* 2018;**130**:177−84.
116. Ma MH, Zhang P, Liang X, Cui DX, Shao QY, Zhang HB, et al. R11 peptides can promote the molecular imaging of spherical nucleic acids for bladder cancer margin identification. *Nano Res* 2022;**15**:2278−87.
117. Hsieh JT, Zhou J, Gore C, Zimmern P. R11, a novel cell-permeable peptide, as an intravesical delivery vehicle. *BJU Int* 2011;**108**:1666−71.
118. Taipaleenmäki E, Städler B. Recent advancements in using polymers for intestinal mucoadhesion and mucopenetration. *Macromol Biosci* 2020;**20**:e1900342.
119. Qi A, Wang CY, Ni SB, Meng YY, Wang TD, Yue ZQ, et al. Intravesical mucoadhesive hydrogel induces chemoresistant bladder cancer ferroptosis through delivering iron oxide nanoparticles in a three-tier strategy. *ACS Appl Mater Inter* 2021;**13**:52374−84.
120. Li W, Liu DF, Zhang HB, Correia A, Mäkilä E, Salonen J, et al. Microfluidic assembly of a nano-in-micro dual drug delivery platform composed of halloysite nanotubes and a pH-responsive polymer for colon cancer therapy. *Acta Biomater* 2017;**48**:238−46.
121. Yuan Y, Liu Y, He Y, Zhang BK, Zhao L, Tian SM, et al. Intestinal-targeted nanotubes-in-microgels composite carriers for capsaicin delivery and their effect for alleviation of Salmonella induced enteritis. *Biomaterials* 2022;**287**:121613.
122. Zheng B, Liu ZH, Wang H, Sun L, Lai WF, Zhang HB, et al. R11 modified tumor cell membrane nanovesicle-camouflaged nanoparticles with enhanced targeting and mucus-penetrating efficiency for intravesical chemotherapy for bladder cancer. *J Control Release* 2022;**351**:834−46.
123. Le-Vinh B, Steinbring C, Wibel R, Friedl JD, Bernkop-Schnürch A. Size shifting of solid lipid nanoparticle system triggered by alkaline phosphatase for site specific mucosal drug delivery. *Eur J Pharm Biopharm* 2021;**163**:109−19.
124. Bonengel S, Prüfert F, Perera G, Schauer J, Bernkop-Schnürch A. Polyethylene imine-6-phosphogluconic acid nanoparticles—a novel zeta potential changing system. *Int J Pharm* 2015;**483**:19−25.
125. Le-Vinh B, Le NN, Nazir I, Matuszczak B, Bernkop-Schnürch A. Chitosan based micelle with zeta potential changing property for effective mucosal drug delivery. *Int J Biol Macromol* 2019;**133**:647−55.